

DEVELOPMENT OF A HYDROPHILIC INTERACTION LIQUID CHROMATOGRAPHY
(HILIC) METHOD FOR THE CHEMICAL CHARACTERIZATION OF WATER-SOLUBLE
ISOPRENE EPOXYDIOL (IEPOX)-DERIVED SECONDARY ORGANIC AEROSOL

Zhexi Zeng

A thesis submitted to the faculty at the University of North Carolina at Chapel Hill in partial fulfillment of the requirements for the degree of Master of Science in the Department of Environmental Sciences and Engineering in the Gillings School of Global Public Health.

Chapel Hill
2018

Approved by:

Jason D. Surratt

Avram Gold

Barbara J. Turpin

© 2018
Zhexi Zeng
ALL RIGHTS RESERVED

ABSTRACT

Zhexi Zeng: Development of a Hydrophilic Interaction Liquid Chromatography (HILIC) Method for the Chemical Characterization of Water-Soluble Isoprene Epoxydiol (IEPOX)-Derived Secondary Organic Aerosol
(Under the direction of Jason D. Surratt)

Atmospheric fine particulate matters ($PM_{2.5}$) adversely affects air quality and human health. Isoprene is the most abundant non-methane volatile organic compound primarily emitted from biogenic sources to Earth's atmosphere. Atmospheric oxidation of isoprene yields large quantities of gaseous isoprene epoxydiol (IEPOX) by hydroxyl radicals under low-nitric oxide conditions. IEPOX subsequently undergoes acid-catalyzed multiphase chemistry with natural or anthropogenic sulfate aerosol, producing substantial amounts of water-soluble IEPOX-derived secondary organic aerosol (SOA) in $PM_{2.5}$. The hydrophilic interaction liquid chromatography interfaced to electrospray ionization-high-resolution quadrupole time-of-flight mass spectrometry (HILIC/ESI-HR-QTOFMS) method presented here overcomes limitations of commonly utilized analytical techniques, making it possible to identify and quantify water-soluble SOA constituents by a single analytical method. Atmospheric chemistry model predictions of the water-soluble IEPOX-derived SOA constituents (e.g., 2-methyltetrols and methyltetrol sulfates) in $PM_{2.5}$ can now be assessed with greater accuracy and confidence.

To all members of the Surratt Research Group. I could't have done this without your support.
Thank you for the collaboration on this work.

ACKNOWLEDGMENTS

This work was funded by the National Science Foundation (NSF) under Atmospheric and Geospace (AGS) Grant 1703535. This work was also supported in part by the NSF under Chemistry (CHE) Grant 1404644, and CAPES Foundation by Brazil Ministry of Education, Brasilia, DF 70.040-020, Brazil. The UNC Biomarker Mass Spectrometry Facility, which contains the HILIC/ESI-HR-QTOFMS instrument, is supported by the National Institute for Environmental Health Sciences (NIEHS) Grant 5P20-ES1012.

TABLE OF CONTENTS

LIST OF TABLES.....	viii
LIST OF FIGURES.....	ix
LIST OF SYMBOLS AND ABBREVIATIONS.....	x
CHAPTER 1: INTRODUCTION.....	1
CHAPTER 2: EXPERIMENT SECTION.....	5
2.1 Synthesized Chemicals.....	5
2.1.1 <i>Trans</i> - β - and δ -IEPOX.....	5
2.1.2 IEPOX-Derived SOA Standards: 2-methyltetrols, 2-methyltetrol sulfates, and 3-methyltetrol sulfates.....	5
2.2 Ultra-Performance Liquid Chromatography/Electrospray Ionization- High Resolution Quadrupole Time-of-Flight Mass Spectrometry (UPLC/ESI-HR-QTOFMS) Analysis.....	6
2.3 Laboratory-Generated SOA from β - and δ -IEPOX.....	7
2.4 Field Sample Collection of PM _{2.5}	9
2.4.1 Look Rock, Tennessee, Southeastern U.S.....	9
2.4.2 Manaus, Brazil, Central Amazonia.....	9
2.5 Sample Preparation for Offline Analyses.....	10

2.5.1 2-Methyltetrol and Methyltetrol Sulfate Standards.....	10
2.5.2 Laboratory-Generated IEPOX SOA Samples.....	10
2.5.3 Field Samples.....	11
CHAPTER 3: RESULT AND DISCUSSION.....	12
3.1 Characterization of IEPOX-Derived SOA Standards.....	12
3.2 Characterization of Laboratory-Generated SOA and Ambient PM _{2.5} Samples.....	13
3.3 Quantification of 2-Methyltetrols and Methyltetrol Sulfates in Laboratory-Generated SOA and Ambient PM _{2.5} Samples.....	15
3.4 Other Measurable Water-Soluble Organic Compounds in Ambient PM _{2.5}	18
3.5 Discrepancy between HILIC/ESI-HR-QTOFMS and GC/EI-MS – Thermal Degradation of Organosulfates.....	18
CHAPTER 4: CONCLUSION.....	21
APPENDIX 1: SUPPLEMENTARY FIGURES.....	31
APPENDIX 2: SUPPLEMENTARY TABLES AND INFORMATION.....	37
APPENDIX 3: METHOD DEVELOPMENT PROCEDURE.....	42
APPENDIX 4: ABSTRACT PROTOCOL OF HILIC/ESI-HR-QTOFMS METHOD.....	44
REFERENCES.....	49

LIST OF TABLES

Table 1 - Properties of the 2-methyltetrol, 2-methyltetrol sulfate and 3-methyltetrol sulfate standards.....	23
Table 2 - Concentrations and mass fractions of 2-methyltetrols and methyltetrol sulfates from samples by HILIC/ESI-HR-QTOFMS.....	24
Table 3 - Concentrations and discrepancies of 2-methyltetrols measured by HILIC/ESI-QTOFMS and GC/EI-MS.....	25

LIST OF FIGURES

Figure 1 - Extracted ion chromatograms (EICs) of methyltetrol sulfates from an RPLC C ₁₈ column and a HILIC BEH amide column.....	26
Figure 2 - EICs of 2-methyltetrols and methyltetrol sulfates from standards and samples.....	27
Figure 3 - EICs of methyltetrol sulfate monomers and dimers from Laboratory-generated SOA samples.....	28
Figure 4 - EICs of other water-soluble organosulfates.....	29
Figure 5 - GC/EI-MS EICs of C5-alkene triols from standards and samples.....	30

LIST OF SYMBOLS AND ABBREVIATIONS

ACN	Acetonitrile
ACSM	Aerodyne Aerosol Chemical Speciation Monitor
BMI	Brechtel Manufacturing Incorporated
DMA	Differential Mobility Analyzer
EC	Elemental Carbon
EIC	Extracted Ion Chromatogram
FIGAERO-CIMS	Filter Inlet for Gases and Aerosol coupled to a Chemical Ionization Mass Spectrometer
GC/EI-MS	Gas Chromatography interfaced to Electron Ionization Mass Spectrometry
HILIC	Hydrophilic Interaction Liquid Chromatography
^1H NMR	Proton Nuclear Magnetic Resonance
HPLC	High-performance Liquid Chromatography
HR-TOF-CIMS	High-resolution Time-of-flight Chemical Ionization Mass Spectrometer
IEPOX	Isoprene Epoxydiol
IMS	Ion Mobility Spectrometry
LC/ESI-HR-MS ⁿ	Liquid Chromatography interfaced to High-resolution Tandem Mass Spectrometry with Electrospray Ionization

LOD	Limit of Detection
LOQ	Limit of Quantification
MCPC	Mixing Condensation Particle Counter
MW	Molecular Weight
m/z	mass to charge ratio
NO	Nitric Oxide
NPLC	Normal Phase Liquid Chromatography
OA	Organic Aerosol
OC	Organic Carbon
PILS	Particle-into-liquid Sampler
PM _{2.5}	Atmospheric fine particulate matter with diameter less than or equal to 2.5 mm
POA	Primary Organic Aerosol
QTOFMS	Quadrupole Time-of-Flight Mass Spectrometry
RPLC	Reverse Phase Liquid Chromatography
RT	Retention time
SEMS	Scanning Electrical Mobility System

SOA	Secondary Organic Aerosol
SOAS	Southern Oxidant and Aerosol Study
SV-TAG	Semi-volatile Thermal Desorption Aerosol Gas Chromatogram
TIC	Total Ion Chromatogram
UPLC	Ultra Performance Liquid Chromatography
VOC	Volatile Organic Compound

CHAPTER 1: INTRODUCTION

Atmospheric fine particulate matter (PM_{2.5}, aerosol particles with aerodynamic diameters $\leq 2.5 \mu\text{m}$), adversely affects air quality. High concentrations of PM_{2.5} can lead to degradation of outdoor visibility¹ and adversely affect human health through cardiovascular and respiratory diseases.² Moreover, atmospheric PM_{2.5} plays a critical role in climate change through both direct and indirect mechanisms.³ Organic aerosol (OA) constituents are recognized to contribute a substantial fraction of PM_{2.5} mass from urban to remote regions around the world.⁴ OA is further characterized into primary organic aerosol (POA) and secondary organic aerosol (SOA). POA is directly emitted in the particle phase from sources, such as sea spray, wildfires, automobiles and cooking, while SOA is formed from the atmospheric oxidation of volatile organic compounds (VOCs) emitted by both anthropogenic and natural sources. Specifically, low-volatility oxidation products from VOCs either nucleate or condense onto existing particles and undergo multiphase chemistry to form SOA. SOA is estimated to contribute up to 70-90% of OA mass found within PM_{2.5}.⁵

Isoprene is the most abundant non-methane hydrocarbon emitted into Earth's atmosphere and is derived largely from deciduous trees.⁶ The atmospheric oxidation of isoprene plays an important role in both tropospheric ozone (O₃)⁷ and SOA formation in forested regions affected by anthropogenic activities.⁸⁻¹⁴ The hydroxyl radical (OH)-initiated oxidation of isoprene during the daytime under low-nitric oxide (NO) conditions produces substantial amounts of isoprene epoxydiols (IEPOX) (~50% yield).^{15,16} The acid-catalyzed multiphase chemistry (reactive

uptake) of IEPOX onto anthropogenic sulfate particles have been shown to produce SOA constituents including 2-methyltetrols,^{8,9,17,18} C₅-alkene triols,^{8,9,17,18} 3-methyltetrahydrofuran-3,4-diols (3-MeTHF-3,4-diols),⁹ organosulfates,^{9,18,19,20} and oligomers.^{9,18,21} Studies have demonstrated that the acidity of sulfate aerosol plays a critical role in forming atmospheric IEPOX-derived SOA.^{22,23}

Protocols for chemical characterization of IEPOX-derived SOA C₅ tracers, including the 2-methyltetrols, C₅-alkene triols, and 3-MeTHF-3,4-diols, have generally employed gas chromatography interfaced to electron ionization mass spectrometry (GC/EI-MS) with prior trimethylsilylation.^{8,9,17-19,24} Volatility and composition analysis by a Filter Inlet for Gases and Aerosol coupled to a Chemical Ionization Mass Spectrometer (FIGAERO-CIMS) equipped with iodide reagent ion chemistry demonstrated that IEPOX-derived SOA has lower volatility in nature and the majority of commonly reported IEPOX SOA C₅ tracers, in particular the 2-methyltetrols, C₅-alkene triols and 3-MeTHF-3,4-diols, are likely derived from the thermal decomposition of accretion products (oligomers) or other low-volatility organics such as organosulfates.²⁵ A second set of studies using semi-volatile thermal desorption aerosol gas chromatogram (SV-TAG) instrumentation with online derivatization reached a similar conclusion.^{26,27} Different protocols, based on liquid chromatography interfaced to high-resolution tandem mass spectrometry with electrospray ionization (LC/ESI-HR-MSⁿ), have been used to characterize organosulfates and oligomers. However, separation of polar, water-soluble components is conventionally attempted with reverse-phase liquid chromatography (RPLC) columns.^{8,9,19,28} RPLC columns do not resolve such compounds well because of either extremely short retention times (RTs), poor peak shapes, or ion suppression effects due to co-eluting inorganic aerosol constituents, leading to potential complications in identifying and quantifying

target compounds. The IEPOX-derived polyols are hydrophilic compounds owing to their hydroxyl functional groups, and the organosulfates are ionic polar compounds.^{12,28} Hence, an alternative approach for the IEPOX-derived SOA characterization that could accomplish simultaneous analysis of polar and water-soluble components while avoiding the drawbacks associated with current analytical methods would be highly desirable.

Hydrophilic interaction chromatography (HILIC) is as an alternative LC method to RPLC to separate hydrophilic (i.e., water-soluble) compounds, including peptides and nucleic acids²⁹ and has recently been reported to separate water-soluble organosulfates with excellent resolution.³⁰⁻³² The HILIC solid phase can be silica gel with a decreased surface concentration of silanol groups, or silica chemically bonded to polar groups, such as amino, amido, cyano, carbamate, diol, polyol, or zwitterionic sulfobetaine groups.³³ A HILIC column separates analytes by forming a water-rich layer, which is partially immobilized around the hydrophilic ligands on the stationary phase. Analytes can undergo partitioning between the bulk organic eluents and the water-rich layer to separate based on different levels of retention.³⁴ Although retention order on HILIC columns is similar to that on normal phase liquid chromatography (NPLC) columns, HILIC utilizes more polar mobile phases (e.g., acetonitrile and Milli-Q water) than the NPLC so that the HILIC method is compatible for interfacing with ESI-MS sources.³⁵ ESI is a soft ionization detection method not involving sample heating or derivatization and is appropriate for detection of polar C₅ tracers, and oligomers as well as water-soluble organosulfates. Based on the demonstrated success of HILIC in the chemical characterization of organosulfates,^{30,31} we undertook development of a HILIC/ESI-HR-quadrupole time-of-flight mass spectrometry (HILIC/ESI-HR-QTOFMS) method for the simultaneous separation, characterization, and quantitation of water-soluble IEPOX-derived SOA constituents from

laboratory-generated β -IEPOX and δ -IEPOX SOA as well as PM_{2.5} collected from the southeastern U.S. and central Amazonia. The HILIC/ESI-HR-QTOFMS protocol developed here can resolve IEPOX-derived 2-methyltetrols, methyltetrol sulfates and oligomers thereof, allowing unambiguous identification and quantification. Current atmospheric models explicitly simulate SOA from the acid-catalyzed multiphase chemistry of IEPOX (i.e., the formation of 2-methyltetrols and methyltetrol sulfates),³⁶⁻³⁹ and the accurate quantification of the 2-methyltetrols and the derived organosulfates will increase confidence in evaluation of model predictions, which will in turn lead to improved modeling. Improvement in quantification of organosulfates will additionally provide much needed data for establishing carbon and sulfur mass closure in IEPOX-derived SOA measured or predicted during future lab and field studies.

CHAPTER 2: EXPERIMENTAL SECTION

2.1 Synthesized Chemicals

2.1.1. *Trans*- β - and δ -IEPOX

Trans- β -IEPOX (trans-2-methyl-2,3-epoxybutane-1,4-diol) and δ -IEPOX (3-methyl-3,4-epoxy-1,2-butanediol) were synthesized in-house according to published methods.^{40,41}

2.1.2. IEPOX-Derived SOA Standards: 2-methyltetrols, 2-methyltetrol sulfates, and 3-methyltetrol sulfates

Diastereomeric mixtures of racemic 2-methyltetrols (racemic 2-methylerythritol and 2-methylthreitol, molecular weight (MW) = 136 g mol⁻¹) were synthesized by acid hydrolysis of δ -IEPOX according to the procedure described in Bondy et al.⁴⁰ 2-Methyltetrol sulfate (MW = 216 g mol⁻¹) was synthesized from 2-methyltetrol. Briefly, 2-methyltetrol was partially acetylated with acetyl anhydride, the desired product, acetylated on the primary and secondary hydroxyl groups, was isolated by column chromatography on SiO₂, eluted with ethyl acetate and then sulfated by a published procedure.³⁰ The protecting acetyl groups were then removed by treatment with ammonia to afford the expected product 2-methyltetrol sulfate. The purity of the 2-methyltetrol sulfate was determined by proton nuclear magnetic resonance (¹H NMR) spectroscopy analysis to be ~100%, with the balance being (NH₄)₂SO₄ (Figure S1). The 3-methyltetrol sulfate (MW = 216 g mol⁻¹) was prepared from δ -IEPOX by a procedure described in Bondy et al.⁴⁰ Briefly, to an ice-cold solution of δ -IEPOX in acetonitrile, Bu₄NHSO₄ and a small amount of potassium bisulfate were added and the reaction allowed to warm to room

temperature and stirred overnight. The resulting mixture of sulfate esters was purified on a Dowex 50W x 4-100 ion exchange column. The final product contained 95.5% 3-methyltetrol sulfates by ^1H NMR analysis with the balance being K_2SO_4 , instead of NaSO_4 in Bondy et al.⁴⁰

2.2 Ultra-Performance Liquid Chromatography/Electrospray Ionization-High Resolution Quadrupole Time-of-Flight Mass Spectrometry (UPLC/ESI-HR-QTOFMS) Analysis

An Agilent 6520 Series Accurate Mass Q-TOFMS instrument (Agilent Technologies), equipped with an ESI source operated in the negative (-) ion mode, was used to chemically characterize IEPOX-derived SOA standards, as well as lab and field samples. Optimum ESI conditions were: 3500 V capillary voltage, 130 V fragmentor voltage, 65 V skimmer voltage, 300 °C gas temperature, 10 L min⁻¹ drying gas flow rate, 35 psig nebulizer, 25 psig reference nebulizer. ESI-QTOFMS mass spectra were recorded from mass-to-charge ratio (m/z) 60 to 1000. HILIC separations were carried out using a Waters ACQUITY UPLC BEH Amide column (2.1 × 100 mm, 1.7 μm particle size, Waters Corp.) at 35 °C. The mobile phases consisted of eluent (A) 0.1% ammonium acetate in water, and eluent (B) 0.1% ammonium acetate in a 95:5 (v/v) acetonitrile (ACN, HPLC Grade, 99.9%, Fisher Scientific)/Milli-Q water. Both eluents were adjusted to a pH of 9 with ammonium hydroxide (NH_4OH). The gradient elution program was eluent A, 0% for 4 min, increasing to 15% from 4 to 20 min, constant at 15% between 4 and 24 min, decreasing to 0% from 24 to 25 min, and constant at 0% from 25 to 30 min. The flow rate and sample injection volume were 0.3 mL min⁻¹ and 5 μL, respectively. Data were acquired and analyzed by Mass Hunter Version B.06.00 Build 6.0.633.0 software (Agilent Technologies). At the beginning of each analysis period, the mass spectrometer was calibrated using a commercially available ESI-L low-mass concentration tuning mixture (Agilent Technologies) in a 95:5 (v/v) ACN/Milli-Q water. Instrument mass axis calibration was conducted in the low-

mass range ($m/z < 1700$). Seven masses were used for calibration: m/z 68.9958, 112.9856, 301.9981, 601.9790, 1033.9881, 1333.9689, and 1633.9498. The adduct of hexakis (1H,1H,3H-tetrafluoropropoxy) phosphazene + acetate (m/z 980.0164), purine (m/z 119.0363), and leucine enkephalin (m/z 554.2620) were continuously infused for real-time mass axis correction. The mass resolution of the ESI-HR-QTOFMS was approximately 8,000-12,300 from m/z 113-1600. For comparison purposes, RPLC separations (Waters ACQUITY UPLC HSS T3 C₁₈ column, 2.1 × 100 mm, 1.8 μm particle size) were also conducted on selected samples that were analyzed by HILIC. The detailed operating procedures for RPLC separations have been described elsewhere.⁴²

2.3 Laboratory-Generated SOA from β- and δ-IEPOX

As described previously, SOA from acid-catalyzed reactive uptake of *trans*-β-IEPOX or δ-IEPOX was generated in the 10-m³ indoor environmental smog chamber at the University of North Carolina. The experimental setup and analysis techniques used in this work were described in detail previously.^{9,23} Briefly, experiments were carried out under dark and wet conditions (50-55%, RH) at 295 ± 1 K. Prior to each experiment, the chamber was flushed continuously with clean air for ~24 hours corresponding to a minimum of seven chamber volumes until the particle mass concentration was < 0.01 μg m⁻³ to ensure that there were no pre-existing aerosol particles. Chamber flushing also reduced VOC concentrations below the detection limit of an iodide-adduct high-resolution time-of-flight chemical ionization mass spectrometer (HR-TOF-CIMS). Operating details of the HR-TOF-CIMS have been previously described.²³ Temperature and RH in the chamber were continuously monitored using a dew point meter (Omega Engineering Inc.). Acidic ammonium sulfate seed aerosol was injected into the pre-humidified chamber using a custom-built atomizer with an aqueous solution of 0.06 M (NH₄)₂SO₄ (aq) and 0.06 M H₂SO₄

(aq) until the desired total aerosol concentration ($\sim 75 \mu\text{m}^3 \text{cm}^{-3}$) was achieved. After seed injection, the chamber was left static for at least 30 min to ensure that the seed aerosol was stable and uniformly mixed. Then, 30 mg of *trans*- β - or δ -IEPOX was injected into the chamber at 2 L min^{-1} for 10 min and then 4 L min^{-1} for 50 min by passing high-purity N_2 (g) through a heated manifold (60°C) containing an ethyl acetate solution of one of the IEPOX isomers described in section 2.1.1.

On completion of IEPOX injection, a filter sample was collected for the subsequent offline analysis using HILIC (or RPLC)/ESI-HR-QTOFMS. Aerosols were collected onto a 46.2 mm Teflon filter ($0.2 \mu\text{m}$, Pall Scientific) in a stainless-steel filter holder for 30 min at a flow rate of 13.2 L min^{-1} . The filter sample along with a blank filter taken from the same batch on the day of the experiment were stored in a 20 mL scintillation vial at -20°C prior to extraction and analysis. In addition to the filter sampling, SOA generated from the reactive uptake of IEPOX was collected using a particle-into-liquid sampler (PILS, Model 4001, Brechtel Manufacturing Inc. - BMI) system at the end of each experiment. The aerosols were sampled through an organic vapor denuder (Sunset Laboratory Inc.) and a $2.5\text{-}\mu\text{m}$ size-cut pre-impactor at a flow rate of $\sim 12.5 \text{ L min}^{-1}$. The sample air flow was then mixed adiabatically with a steam flow heated at $98.5\text{-}100^\circ \text{C}$ in the PILS condensation chamber to produce high supersaturation of water vapor that grow particles to collectable sizes for collection onto a quartz impactor plate by inertial impaction. Impacted droplets were transferred by a wash-flow at $\sim 0.55 \text{ mL min}^{-1}$ through a debubbler and the resulting bubble-free sample liquid was delivered through a tubing with an inline filter into 2-mL poly vials held on an auto-collector (BMI) with a rotating carousel. Air sampling rate and wash-flow rate were examined and recorded before and after each experiment. Milli-Q water used in the wash-flow was spiked with $25 \mu\text{M}$ lithium bromide (LiBr, Sigma-

Aldrich, 99.5%) as an internal standard to correct for dilution caused by condensation of water vapor during droplet collection. The dilution factor was typically from 1.1-1.2. The PILS vials were promptly stored under dark conditions at 2 °C upon collection until analysis. Chamber aerosol number distributions, which were subsequently converted to total aerosol surface area and volume concentrations, were monitored by a scanning electrical mobility system (SEMS v5.0, BMI) containing a differential mobility analyzer (DMA, BMI) coupled to a mixing condensation particle counter (MCPC, Model 1710, BMI), in order to estimate the total aerosol mass. Summary of the experimental conditions can be found in Table S1.

2.4 Field Sample Collection of PM_{2.5}

2.4.1 Look Rock, Tennessee, Southeastern U.S.

Quartz filter samples of PM_{2.5} were collected at a field site (Look Rock, Tennessee, USA) during the Southern Oxidant and Aerosol Study (SOAS) campaign in Summer 2013 by a previously described procedure.¹² The filters were stored in the dark in a -20 °C walk-in freezer until chemical analysis. The sample selected for re-analysis was collected for three hours (16:00-19:00 local time) when one of the highest isoprene-derived SOA concentrations was measured during the campaign.^{12,13}

2.4.2 Manaus, Brazil, Central Amazonia

PM_{2.5} samples were collected from November 28 - December 1 (transition of dry-to-wet season), 2016 on pre-baked Tissuquartz Filters (Whatman, 20 cm × 25 cm) using a high-volume PM_{2.5} sampler (ENERGÉTICA with PM_{2.5} Size Selective Inlet) located in the School of Technology of the Amazonas State University in Manaus, Brazil, near a major road. The high-volume PM_{2.5} sampler was located 6 m above the ground and was equipped with a cyclone operated at 1.13 m³ min⁻¹. Sampler was flow calibrated and the filter holder was cleaned with the

filter extraction solvent each day before sampling to ensure no carryover between samples. All filters were pre-baked for 12 h at 550 °C and all samples were collected for 24 h (total sampling volume of 1527.81 m³). PM_{2.5} mass was determined by weighing filters before and after sampling following equilibration at 21 ± 2 °C for 24 hours after equilibrating under < 50% RH. Filters were stored at -18 °C in the dark until analysis. Similar to the sample selected from Look Rock, one sample (i.e., November 30, 2016) selected for re-analysis had the highest loading of PM_{2.5} and IEPOX-derived SOA tracers (e.g. 2-methyltetrols and C₅-alkene triols) measured by GC/EI-MS among all samples. GC/EI-MS analysis with prior derivatization of selected samples as a comparison was performed following the procedures described previously.⁹

2.5 Sample Preparation for Offline Analyses

2.5.1 2-Methyltetrol and Methyltetrol Sulfate Standards

The 2-methyltetrol, 2-methyltetrol sulfate and 3-methyltetrol sulfate standards were stored at -20 °C until being dissolved in a 2 mg mL⁻¹ Milli-Q water solution, and then serially diluted immediately with 95:5 (v/v) ACN/Milli-Q water to 50, 10, 1, 0.25, 0.1, 0.025, and 0.01 µg mL⁻¹ standards. The diluted standards were kept at 4 °C and analyzed within 24 h of preparation.

2.5.2 Laboratory-Generated IEPOX SOA Samples

Blank and sample filters of SOA generated from β-IEPOX and δ-IEPOX were immersed in 22 mL of methanol and extracted for 45 min by ultra-sonication. The extracts were filtered through polypropylene membrane syringe filters and the solvent was evaporated under a gentle stream of nitrogen gas. Half of the dried methanol extracts were reconstituted with 150 µL of 95:5 (v/v) ACN/Milli-Q water and then diluted by a factor of 100 or 50, respectively for the β-IEPOX- and δ-IEPOX-derived SOA samples, in order to prepare the methyltetrol sulfates in the

linear range of the calibration curves. The concentrations of the methyltetrol sulfates in the 150 μL reconstituted solutions were not saturated and estimated later to be 360-410 $\mu\text{g mL}^{-1}$, which were much lower than the solubility of the methyltetrol sulfates that were determined to be at least 2500 $\mu\text{g mL}^{-1}$; specifically, maximum solubility was determined by dissolving 25 mg of the methyltetrol sulfate standards in 10 mL of 95:5 (v/v) of acetonitrile and Milli-Q water. The aqueous PILS samples collected for the laboratory-generated IEPOX SOA near the end of the experiment were diluted by a factor of 20 using ACN in order to prepare them in 95:5 (v/v) ACN/water, and promptly analyzed using the HILIC/ESI-HR-QTOFMS method without any further pretreatment.

2.5.3 Field Samples

A 37-mm-diameter punch from the quartz filter from Look Rock along with a lab blank filter were extracted as described above. Half of the Look Rock $\text{PM}_{2.5}$ extract was reconstituted with 150 μL of 95:5 (v/v) ACN/Milli-Q water and then diluted by a factor of 20.

Similarly, a 47-mm diameter punch from the selected quartz filter from Manaus, Brazil, as well as a lab blank filter, was extracted as described above. The residues were reconstituted in 1 mL methanol and a 0.3 mL aliquot was dried and reconstituted in 150 μL of 95:5 (v/v) ACN/Milli-Q water, and then diluted by a factor of 30 for analysis by HILIC/ESI-HR-QTOFMS.

CHAPTER 3: RESULT AND DISCUSSION

3.1 Characterization of IEPOX-Derived SOA Standards

Figure 1 compares the extracted ion chromatograms (EICs) of the ionized 2- and 3-methyltetrol sulfate standards separated by RPLC and HILIC columns coupled to the ESI-HR-QTOFMS. On the RPLC column, both methyltetrol sulfate standards co-elute as one peak at 1.5 min (Figure 1, a1-a2). By contrast, the HILIC protocol is able to resolve four or six chromatographic peaks for the 2- and 3-methyltetrol sulfate standards, respectively (Figure 1, b1-b2, also in Figure 2, b1). Comparison of the total ion chromatograms (TICs) acquired by RPLC and HILIC from an IEPOX-derived SOA in Figure S2, along with Figure 1 (b1-b2), unequivocally demonstrates the superiority of HILIC for separating and quantifying the multiple isomers of organosulfates derived from IEPOX.

Calibration curves were established using authentic standards of 2-methyltetrols, 2- and 3-methyltetrol sulfates. Figure 2 (a1) shows that the deprotonated 2-methyltetrol diastereomers eluted at an identical retention time (RT) of 4.0 min using the HILIC column. By contrast, GC/EI-MS analysis with prior derivatization resolved the 2-methyltetrols diastereomers.^{8,9,18,24} However, HILIC protocol is able to resolve 2- and 3-methyltetrol sulfates diastereomers not resolvable by GC/EI-MS. As shown in Figure 2 (b1, dashed line), four isomeric peaks with RTs of 2.1, 2.6, 4.2, and 5.2 min, were resolved at m/z 215.023 on the EIC corresponding to the 2-methyltetrol sulfate standard, while six peaks with RTs of 2.1, 2.6, 4.2, 5.2, 8.0, and 8.3 min, were resolved from the 3-methyltetrol sulfate standard in Figure 2 (b1, solid line). Importantly, the 2-methyltetrols were simultaneously detected and chromatographically resolved with the

methylethanol sulfates. To our knowledge, this HILIC/ESI-HR-QTOFMS method represents the first time that the major IEPOX-derived SOA constituents, confirmed by authentic 2-methylethanol, 2- and 3-methylethanol sulfates, have been chromatographically resolved and characterized by a single mass spectrometric technique operated with one column and ionization mode.

The linear dynamic range for the 2-methylethanol was 0.01-25 $\mu\text{g mL}^{-1}$ with a limit of detection (LOD) of 7.74 $\mu\text{g L}^{-1}$ and a limit of quantification (LOQ) of 25.8 $\mu\text{g L}^{-1}$ (Table 1). The linear dynamic range of 2-methylethanol sulfates was 0.01-10 $\mu\text{g mL}^{-1}$, with an LOD of 1.72 $\mu\text{g L}^{-1}$ and an LOQ of 5.75 $\mu\text{g L}^{-1}$. The linear dynamic range of 3-methylethanol sulfates was 0.01-25 $\mu\text{g mL}^{-1}$, with an LOD of 3.83 $\mu\text{g L}^{-1}$ and an LOQ of 12.8 $\mu\text{g L}^{-1}$. R^2 values of the calibration curves ranged from 0.9994-1.0000. The linear dynamic ranges of the organosulfates in this study are broader than those reported by Hettiyadura et al., which ranged from 0.025-0.5 $\mu\text{g mL}^{-1}$.³⁰ The high coefficients of determination (R^2) and low LOQs suggest the high performance of HILIC method is the most effective procedure for quantification of organosulfates in IEPOX-derived SOA.

3.2 Characterization of Laboratory-Generated SOA and Ambient PM_{2.5} Samples

Standard calibration curves of the authentic 2-methylethanol, 2- and 3-methylethanol sulfates were used to identify and quantify tracers. The EICs at m/z 135.066 which correspond to the deprotonated 2-methylethanol resolved on the HILIC column are shown in Figure 2. Figure 2 (a1-a5) compares the EICs of the 10 $\mu\text{g mL}^{-1}$ standards of authentic 2-methylethanol, aerosol filter extracts of laboratory-generated SOA derived from *trans*- β -IEPOX and δ -IPEOX, PM_{2.5} samples from the Look Rock field site during 2013 SOAS campaign and from Manaus, Brazil in November 2016. The chromatographic peak at 4.0 min observed in all samples corresponds to

the 2-methyltetrols. Figure 2 (a1-a5) demonstrates that HILIC/ESI-HR-QTOFMS can unequivocally identify the 2-methyltetrols in laboratory and ambient PM_{2.5} samples.

Figure 2 (b1-b5) compares the EICs at m/z 215.023 of 10 $\mu\text{g mL}^{-1}$ standards of authentic 2- and 3-methyltetrol sulfates, filter samples of laboratory-generated SOA derived from *trans*- β -IEPOX and δ -IEPOX, PM_{2.5} samples collected at the Look Rock site during the 2013 SOAS campaign and from Manaus, Brazil in November 2016, respectively. In the EIC of the 10 $\mu\text{g mL}^{-1}$ 3-methyltetrol sulfate standard (Figure 2, b1, solid line), two predominant isomers eluted at 8.0 and 8.3 min. These two chromatographic peaks were also present as major components from the laboratory-generated δ -IEPOX SOA (Figure 2, b3), and as minor components from the two field samples (Figure 2, b4-b5), but were absent from the 10 $\mu\text{g mL}^{-1}$ standard of the 2-methyltetrol sulfate (Figure 2, b1, dashed line), nor in the laboratory-generated *trans*- β -IEPOX SOA (Figure 3, b2), indicating that these two later-eluting isomers arise from the acid-catalyzed multiphase chemistry of δ -IEPOX. This observation will be helpful in studies to determine the origin and formation pathway of ambient methyltetrol sulfates. Peaks at RTs of 2.1, 2.6, 4.2, and 5.2 min were present in chromatograms of sulfate ester diastereomers of 2- and 3-methyltetrol; however, Figure 2 (b2) shows that the peak at RT 5.2 min was predominant in the EIC of sulfate diastereomers from *trans*- β -IEPOX, suggesting that this diastereomer is indicative of *trans*- β -IEPOX as the source. Full scan mass spectra of selected chromatographic peaks at m/z 215.023 in Figure 2 are shown in Figure S3.

The 2- and 3-methyltetrol sulfates derived from β - and/or δ -IEPOX were present in ambient PM_{2.5} SOA collected at the Look Rock and Manaus field sites (Figure 2, b4-b5). The two diastereomers with the longest RTs (8.0 and 8.3 min), formed from δ -IEPOX and predominant in the 3-methyltetrol sulfate standard, were barely detectable in the ambient aerosol

samples. This observation identifies (*cis*- or *trans*-) β -IEPOX as the predominant ambient IEPOX isomer, accounting for 97% of total ambient IEPOX,¹⁶ which corroborates results based on ESI-ion mobility spectrometry (IMS)-HR-TOFMS as reported by Krechmer et al.⁴³ for the PM_{2.5} collected from the Look Rock site during the 2013 SOAS campaign. Hence, the methyltetrol sulfate isomers at 2.1, 2.6, 4.2, 5.2 min support β -IEPOX isomers as the major contributor to the PM_{2.5} collected at both of the Look Rock and Manaus field sites, which demonstrates the advantage of HILIC/ESI-HR-QTOFMS in differentiation of isomers and apportionment of reaction pathways.^{9,12,18}

3.3 Quantification of 2-Methyltetrols and Methyltetrol Sulfates in Laboratory-Generated SOA and Ambient PM_{2.5} Samples

Concentrations of the 2-methyltetrols and methyltetrol sulfates in the laboratory-generated SOA collected by PILS and ambient PM_{2.5} filters were quantified by HILIC/ESI-HR-QTOFMS and are summarized in Table 2. PILS sampling was chosen to improve mass closure to avoid uncertainty due to filter sampling artifacts and pretreatment steps. Methyltetrol sulfates were quantified by an authentic 2-methyltetrol sulfate standard since the two major chromatographic peaks (RTs at 4.2 and 5.2 min) were consistently predominant in the standard and the PM_{2.5} samples, except that authentic 3-methyltetrol sulfate was used as a standard to quantify methyltetrol sulfate in laboratory-generated SOA from δ -IEPOX. The percentage of 2-methyltetrols and methyltetrol sulfates in total aerosol mass is also shown in Table 2, calculated by dividing the mass concentration of each compound by the total aerosol mass obtained from SEMS-MCPC, assuming a particle density of 1.42 g cm⁻³ for β -IEPOX SOA or 1.55 g cm⁻³ for δ -IEPOX SOA (see electronic supporting information (SI) for details). The analytical uncertainty in the quantification was determined to be up to ~17.2% (SI). As shown in Table 2, the

concentration of the 2-methyltetrols in laboratory-generated *trans*- β -IEPOX-derived SOA was $63.98 \mu\text{g m}^{-3}$ (33.9% of total particle mass) and the concentration of methyltetrol sulfates was $109.67 \mu\text{g m}^{-3}$ (58.2% of total particle mass). In the laboratory-generated SOA from δ -IEPOX, the concentration of the 2-methyltetrols $29.49 \mu\text{g m}^{-3}$ (19.6% of total aerosol mass) and methyltetrol sulfates was $62.98 \mu\text{g m}^{-3}$ (42.0% of total aerosol mass). Together, the two IEPOX-derived SOA tracers contributed 92.1% of the total aerosol mass from β -IEPOX and 61.6 % of the total aerosol mass from δ -IEPOX (Table 2). The methyltetrol sulfates account for approximately twice the 2-methyltetrol mass. The mass fractions of methyltetrol sulfates indicate conversion of a significant amount of inorganic sulfate seed aerosol to organosulfates (Figure S4).

In addition to the monomeric methyltetrol sulfates (m/z 215.023), Figure 3 shows that the HILIC column resolves multiple isomeric methyltetrol sulfate dimers (m/z 333.086) in laboratory SOA generated from β - and δ -IEPOX, suggesting oligomeric products as a likely source of the unaccounted for aerosol mass. RPLC did not resolve isomers of either species (Figure S2).^{9,18} Additionally, small intensities of 2-methyltetrol dimers ($\text{C}_{10}\text{H}_{21}\text{O}_7^-$, $m/z = 253.129$) were detected in ambient samples from Look Rock and Manaus field sites. These dimers were not quantified due to the lack of authentic standards.

In the Look Rock $\text{PM}_{2.5}$ sample, the mass concentration of the 2-methyltetrol was measured by HILIC/ESI-HR-QTOFMS to be $0.86 \mu\text{g m}^{-3}$, accounting for 5.6% of the total OA mass, or 7.5% of the total organic carbon (OC) mass. The total OA mass concentration averaged during the sampling period was determined to be $15.30 \mu\text{g m}^{-3}$ using an Aerodyne Aerosol Chemical Speciation Monitor (ACSM),¹² and the total OC mass concentration from the same sample was measured to be $5.04 \mu\text{gC m}^{-3}$ using a Sunset laboratory OC-elemental carbon (EC)

aerosol analyzer. Methyltetrol sulfates, quantified using the 2-methyltetrol sulfate standard, were determined to be $2.33 \mu\text{g m}^{-3}$, accounting for 15.3% of the total OA (or 12.9% of the total OC) mass, and significantly higher than $1.14 \mu\text{g m}^{-3}$ measured by RPLC/ESI-HR-QTOFMS.¹² This discrepancy suggests that the RPLC/ESI-HR-QTOFMS method likely underestimates the methyltetrol sulfate concentrations, possibly resulting from the lack of proper dilution or appropriate isomeric standards, or caused by ion suppression due to co-elution with other water-soluble organic or inorganic aerosol components. The sum of the 2-methyltetrols and methyltetrol sulfates quantified by the new method accounted for 20.9% of the total OA mass in the Look Rock sample during the 2013 SOAS campaign when high intensity of isoprene and anthropogenic emissions (acidic sulfate aerosol) were observed, making IEPOX-derived SOA the single largest contributor to the characterized OA constituents.¹²

For the Manaus sample, the HILIC/ESI-HR-QTOMS analysis measured 0.14 and $0.39 \mu\text{g m}^{-3}$ for 2-methyltetrols and methyltetrol sulfates, respectively, accounting for 0.74% and 1.34% of the total OC mass concentration ($8.12 \mu\text{gC m}^{-3}$ for this particular sample collected on November 30, 2016) measured by a Sunset laboratory OC-EC aerosol analyzer. In addition, elevated concentrations of levoglucosan ($0.46 \mu\text{g m}^{-3}$ by GC/EI-MS), EC ($1.18 \mu\text{gC m}^{-3}$ by a Sunset OC-EC aerosol analyzer), and $\text{PM}_{2.5}$ ($46.1 \mu\text{g m}^{-3}$) were observed on this particular day, and more generally during the November 28-30, 2016, sampling period due to the large influence of biomass burning. In fact, average levoglucosan, OC, EC, and $\text{PM}_{2.5}$ concentrations during this biomass burning intensive period were $0.41 \mu\text{g m}^{-3}$, $8.0 \mu\text{gC m}^{-3}$, $1.3 \mu\text{gC m}^{-3}$, and $43.6 \mu\text{g m}^{-3}$, respectively. The elevated biomass burning likely explains why the IEPOX-derived SOA tracers accounted for a lower % contribution to the total OC mass versus the southeastern U.S. sample (Table 2), which the latter had little influences of biomass burning.¹²

3.4 Other Measurable Water-Soluble Organic Compounds in Ambient PM_{2.5}

In addition to the targeted analysis for the 2-methyltetrols and methyltetrol sulfates, we were able to detect several other isoprene-derived organosulfates in the ambient PM_{2.5} samples. Figure 4 shows the EICs of organosulfates with chemical formulas C₄H₇O₇S⁻ (*m/z* 199, accurate mass = 198.9912), C₅H₉O₇S⁻ (*m/z* 213, accurate mass = 213.0069), and C₅H₇O₇S⁻ (*m/z* 211, accurate mass = 210.9912) detected in the PM_{2.5} samples from Look Rock and Manaus. These species have also been reported from other field and laboratory studies, including EICs obtained from HILIC/ESI-MS.^{20,30-32} The ion of *m/z* 199 was confirmed as the sulfate ester derived from another isoprene SOA tracer 2-methylglyceric acid in high-NO_x conditions.^{10,45} The structures of the *m/z* 211 and 213 were tentatively proposed with EICs consistent with previous observations.^{20,31,32}

3.5 Discrepancy between HILIC/ESI-HR-QTOFMS and GC/EI-MS – Thermal Degradation of Organosulfates

Table 3 lists the concentrations of 2-methyltetrols in samples of SOA from β-IEPOX, δ-IEPOX, Look Rock, and Manaus quantified in parallel by HILIC/ESI-HR-QTOFMS and GC/EI-MS with prior derivatization. The concentrations of 2-methyltetrols determined by GC/EI-MS were 104, 136, 60, and 188% higher, respectively, than those determined by HILIC/ESI-HR-QTOFMS. The discrepancies are consistent with suggestions that GC/EI-MS overestimates semi-volatile marker compounds because of thermal degradation of low-volatility accretion products (e.g., oligomers or possibly organosulfates).²⁵ To investigate whether the overestimation in fact resulted from thermal degradation or trimethylsilylation of the analytes, calibration curves of 2-methyltetrol, 2- and 3-methyltetrol sulfates were generated by GC/EI-MS along with the four SOA samples. As shown in Figure 5/S5/S6 (b-c), the isoprene-derived SOA

tracers commonly observed by GC/EI-MS, including C₅-alkene triols, 2-methyltetrols, and 3-MeTHF-3,4-diols, were detected in the pure 2- and 3-methyltetrol sulfate standards. Figure S5 (a-c) illustrates the formation of 2-methyltetrols in the GC/EI-MS analysis of the 50 µg mL⁻¹ 2- and 3-methyltetrol sulfate standards. The GC/EI-MS EIC of *m/z* 219 for the 50 µg mL⁻¹ derivatized standard of authentic 2-methyltetrol diastereomer mixture is characterized by peaks at RTs of 34.0 and 34.8 min. Peaks with relative intensities of ~0.25 and ~5% at the same RTs characterize the EICs at *m/z* 219 of the pure 2- and 3-methyltetrol sulfate standards. The 2-methyltetrols from degradation of the organosulfates can partially explain the large discrepancy measured between the HILIC/ESI-HR-QTOFMS and GC/EI-MS methods. Other organosulfates and oligomers present in the aerosol samples may also contribute to the discrepancy. The C₅-alkene triol tracers for isoprene SOA, have been detected only by GC/EI-MS or SV-TAG methods.^{8,9,17,26,44} Lopez-Hilfiker et al.²⁵ have reported that the high concentrations of C₅-alkene triols measured in PM_{2.5} samples analyzed by these procedures, in which samples are treated at high-temperature, are not consistent with their estimated volatility, and suggest that these compounds are degradation products of IEPOX-derived organosulfates and oligomers. Based on the semi-quantitative relationship established for the C₅-alkene triols produced from the 2-methyltetrol sulfate standards prepared (SI), 30.0%, 42.8%, and 14.7% of the C₅-alkene triols measured by GC/EI-MS could be attributed to the potential thermal degradation of the 2-methyltetrol sulfates in the PM_{2.5} samples from laboratory-generated β-IEPOX SOA, Look Rock, and Manaus, respectively (Table S2). Similarly, 11.1% of the 2-methyltetrols and approximately all 3-MeTHF-3,4-diols in laboratory-generated δ-IEPOX SOA may be products of the thermal degradation of the 3-methyltetrol sulfates (Table S3). As demonstrated above, thermal degradation of organosulfates as well as low-volatility accretion aerosol products (i.e.,

oligomers) explain a substantial fraction of the isoprene-derived SOA tracers previously measured through analytical methods such as GC/EI-MS or SV-TAG in which samples are treated at high temperatures.⁴⁶ HILIC/ESI-HR-QTOFMS avoids such treatment and is therefore preferred for accurate quantification of IEPOX-derived SOA constituents.

CHAPTER 4: CONCLUSION

The availability of authentic IEPOX-derived SOA standards was critical in developing the HILIC/ESI-HR-QTOFMS method described here. This protocol was used to evaluate IEPOX-derived SOA samples generated in laboratory studies or PM_{2.5} samples collected from two isoprene-rich regions. The HILIC column can resolve the major water-soluble IEPOX-derived SOA constituents, including the 2-methyltetrols, methyltetrol sulfates and the corresponding dimers that are predicted to form in regional and global scale atmospheric chemistry models.^{36-39,47-49} The major water-soluble IEPOX-derived SOA constituents can be quantified by one method with improved accuracy. We have demonstrated the ability to distinguish between different isomers of β - and δ -IEPOX-derived methyltetrol sulfates, which allows the contribution of the IEPOX isomers to be apportioned with the availability of authentic sulfate standards. Analysis by the HILIC method avoids high-temperatures required by GC/EI-MS or SV-TAG methods which cause degradation of IEPOX-derived organosulfates and oligomers to 2-methyltetrols, C₅-alkene triols, and 3-MeTHF-3,4-diols with consequent distortion of actual product distributions.^{25,49}

By taking advantage of authentic standards and the HILIC/ESI-HR-QTOFMS method, we have estimated the mass fractions of the 2-methyltetrols and the methyltetrol sulfates in laboratory and ambient SOA samples. In summary, these two types of SOA constituents, likely the two largest contributors, contributed 92% and 62% to total aerosol mass, and 21% to OA mass from the laboratory-generated β -IEPOX SOA, laboratory-generated δ -IEPOX SOA, and Look Rock PM_{2.5}, respectively. These two SOA constituents contributed ~2.1% to OC mass

from Manaus PM_{2.5} sample, which was likely lower owing to the fact that biomass burning was a large contributor to the OC mass during this sampling period whereas the Look Rock PM_{2.5} sample had little influences of biomass burning. The methyltetrol sulfates are the largest single contributor to the IEPOX SOA mass, contributing ~2-3 times of the mass of the 2-methyltetrols. The predominant contributions of organosulfates (>90% of the reactive uptake of β -IEPOX) reveal the significance of conversion of inorganic sulfate to organosulfate, and emphasize the importance of the multiphase chemistry of IEPOX leading to SOA formation in the isoprene-rich regions. In addition, oligomers derived from the methyltetrol sulfates and the 2-methyltetrols may explain the missing fraction of the total aerosol mass.

Large abundances of methyltetrol sulfates in atmospheric PM_{2.5} could explain previous observations of the low-volatility nature of IEPOX-derived SOA in ambient aerosol.^{25,50} The HILIC/ESI-HR-QTOFMS procedure described here can resolve water-soluble organic carbons from isoprene photochemical products generated via non-IEPOX pathways. HILIC separation can be interfaced to current RPLC/ESI-HR-QTOFMS procedures to develop two dimensional LC/ESI-HR-QTOFMS, further enhancing resolution of hydrophilic organic compounds in PM_{2.5}.

Table 1. Properties of the 2-methyltetrol, 2-methyltetrol sulfate and 3-methyltetrol sulfate standards characterized by HILIC/ESI-HR-Q-TOFMS, including linearity, coefficient of determination (R^2), limit of detection (LOD), limit of quantification (LOQ), and relative standard deviation (RSD) of ten replicate injections. Note that structures are for one of two diastereomers for each standard and ions are shown for the methyltetrol sulfates.

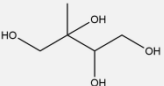
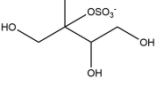
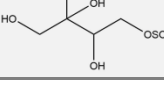
Standards	Chemical Structure	[M-H] ⁻	<i>m/z</i>	Retention Time(s) (min)	Linear Range (µg mL ⁻¹)	R^2	LOD (µg L ⁻¹)	LOQ (µg L ⁻¹)
2-methyltetrols		C ₅ H ₁₁ O ₄ ⁻	135.066	4.0	0.01-25	0.9994	7.74	25.8
2-methyltetrol sulfates		C ₅ H ₁₁ O ₇ S ⁻	215.023	2.1, 2.6, 4.2, 5.2	0.01-10	0.9996	1.72	5.75
3-methyltetrol sulfates		C ₅ H ₁₁ O ₇ S ⁻	215.023	2.1, 2.6, 4.2, 5.2, 8.0, 8.3	0.01-25	1.0000	3.83	12.8

Table 2. Concentrations and mass fractions of 2-methyltetrols and methyltetrol sulfates measured from laboratory-generated SOA and ambient PM_{2.5} samples by HILIC/ESI-HR-QTOFMS.

	2-Methyltetrols		Methyltetrol sulfates	
	Mass Conc. ($\mu\text{g m}^{-3}$) ^a	% Total Mass ^b	Mass Conc. ($\mu\text{g m}^{-3}$)	% Total Mass
Laboratory β -IEPOX SOA	63.98	33.9 %	109.67	58.2 %
Laboratory δ -IEPOX SOA	29.49	19.6 %	62.98	42.0 %
Look Rock, TN	0.861	5.6 (7.5) %	2.334	15.3 (12.9) %
Manaus, Brazil	0.137	(0.74) %	0.390	(1.34) %

^a The mass concentrations of 2-methyltetrols and methyltetrol sulfates were measured from the PILS samples for the laboratory-generated SOA, and from the filter samples for the Look Rock and Manaus samples;

^b The total aerosol mass (organic + inorganic, shown in **bold**) was used for the mass closure for the laboratory-generated SOA, while the organic aerosol (or organic carbon, shown in parentheses) mass was used for the mass closure for the Look Rock and Manaus samples. The total aerosol mass was determined using an SEMS-MCPC system for the laboratory-generated SOAs, assuming the particle density to be 1.42 or 1.55 g cm⁻³ after reaction from β - or δ -IEPOX (SI). The total organic aerosol mass for the Look Rock sample was measured by an ACSM.^{11,12} The OC mass for the Look Rock and Manaus samples was measured using EC/OC analyzers. The relative analytical uncertainty in the quantification was determined to be up to ~17.2% (SI).

Table 3. Concentrations and discrepancies of 2-methyltetrols ($\mu\text{g m}^{-3}$) from laboratory-generated SOA and ambient PM_{2.5} samples measured by HILIC/ESI-QTOFMS and GC/EI-MS.

2-Methyltetrols ($\mu\text{g m}^{-3}$)	HILIC/ESI- QTOFMS	GC/MS	Ratio (GC/HILIC)
Laboratory β -IEPOX SOA	69.05	140.86	204 %
Laboratory δ -IEPOX SOA	51.91	122.56	236 %
Look Rock, TN	0.861	1.381	160 %
Manaus, Brazil	0.137	0.394	288 %

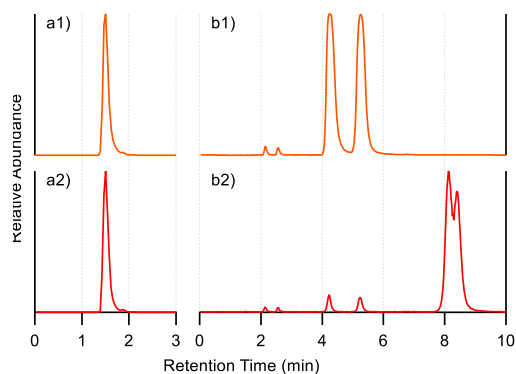


Figure 1. Extracted ion chromatograms (EICs) at m/z 215.023 corresponding to methyltetrol sulfates. Using **a)** RPLC C_{18} column, and **b)** HILIC BEH amide column: standards of 1) 2-methyltetrol sulfates; 2) 3-methyltetrol sulfates. Standards were prepared at $10 \mu\text{g mL}^{-1}$. No significant peaks were observed beyond the shown periods of retention time.

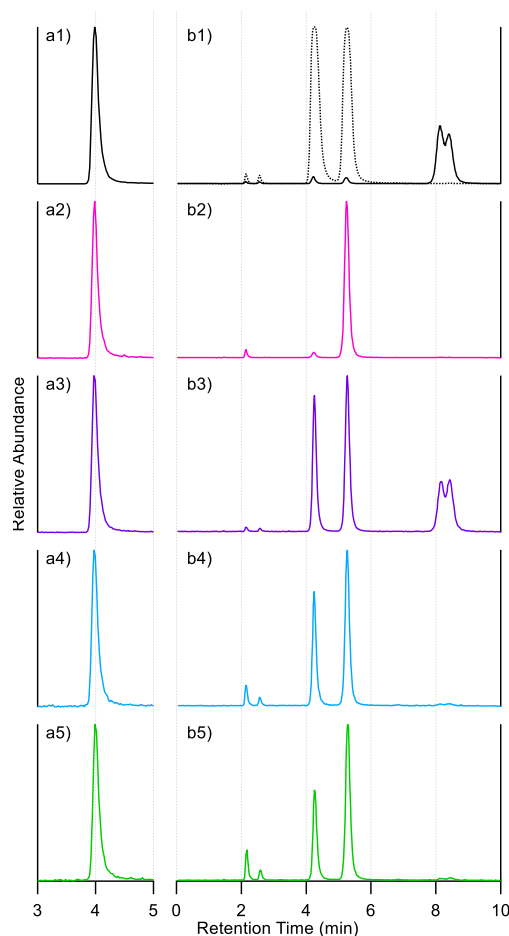


Figure 2. EICs of **a)** m/z 135.066 corresponding to 2-methyltetrols, **b)** m/z 215.023 corresponding to methyltetrol sulfates from: 1) $10 \mu\text{g mL}^{-1}$ synthesized standard (b1: 2-methyltetrol sulfates (dashed line) and 3-methyltetrol sulfates (solid line)); 2) laboratory-generated β -IEPOX SOA; 3) laboratory-generated δ -IEPOX SOA; 4) $\text{PM}_{2.5}$ sample collected at Look Rock during 2013 SOAS campaign; 5) $\text{PM}_{2.5}$ sample collected at Manaus in Nov. 2016. The laboratory-generated β -IEPOX SOA, δ -IEPOX SOA, Look Rock, and Manaus samples were diluted by a factor of 200, 100, 40, and 100, respectively. No significant peaks were observed beyond the shown periods of retention time.

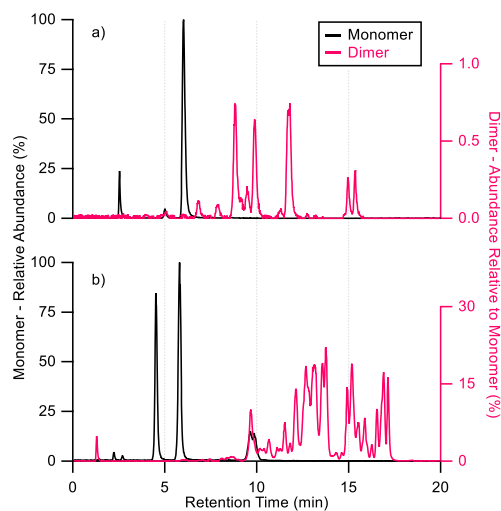


Figure 3. EICs of m/z 215.023 ($C_5H_{11}O_7S^-$) and 333.086 ($C_{10}H_{21}O_{10}S^-$) corresponding to methyltetrol sulfate monomers and dimers, respectively, from **a)** laboratory-generated β -IEPOX SOA diluted by a factor of 200; and **b)** laboratory-generated δ -IEPOX SOA. No significant peaks were observed beyond 20 min.

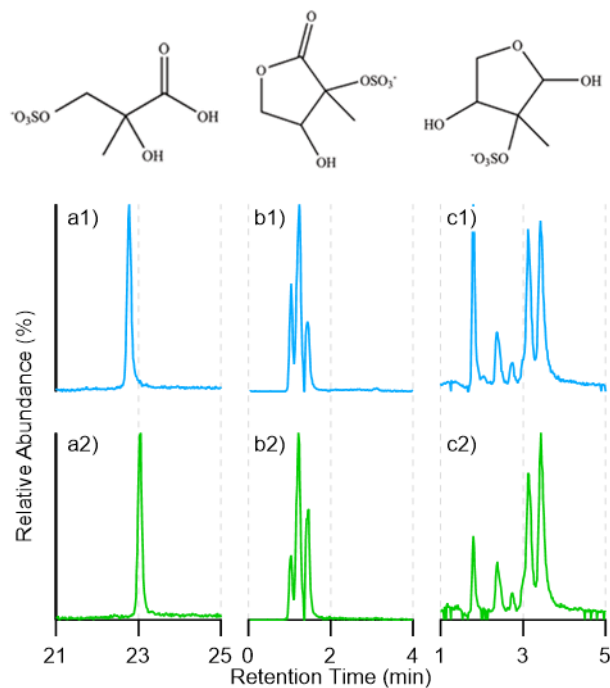


Figure 4. EICs of other water-soluble organosulfates with their proposed structures: **a)** m/z 199 corresponding to $C_4H_7O_7S^-$, **b)** m/z 211 corresponding to $C_5H_7O_7S^-$, and **c)** m/z 213 corresponding to $C_5H_9O_7S^-$ observed in $PM_{2.5}$ samples collected from 1) Look Rock during 2013 SOAS campaign; 2) Manaus in Nov. 2016. No significant peaks were observed beyond the shown periods of retention time.

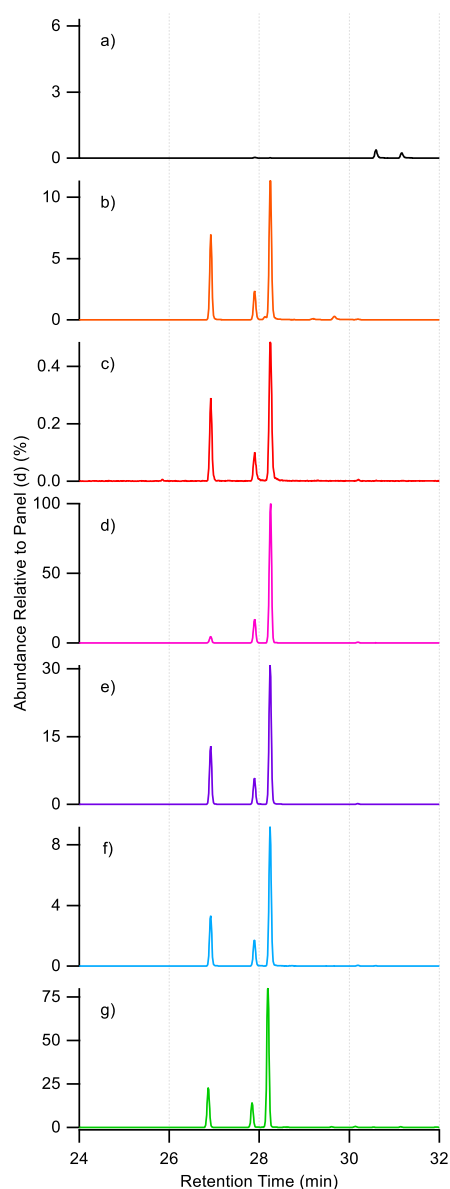


Figure 5. GC/EI-MS EICs of m/z 231 corresponding to C_5 -alkene triols (RT = 26.9, 27.9, 28.3 min) from: **a)** $50 \mu\text{g mL}^{-1}$ standard of 2-methyltetrol; **b)** $50 \mu\text{g mL}^{-1}$ standard of 2-methyltetrol sulfate; **c)** $50 \mu\text{g mL}^{-1}$ standard of 3-methyltetrol sulfate; **d)** laboratory-generated β -IEPOX SOA; **e)** laboratory-generated δ -IEPOX SOA; **f)** $\text{PM}_{2.5}$ sample at Look Rock during 2013 SOAS campaign; **g)** $\text{PM}_{2.5}$ sample at Manaus in Nov. 2016.

APPENDIX 1: SUPPLEMENTARY FIGURES

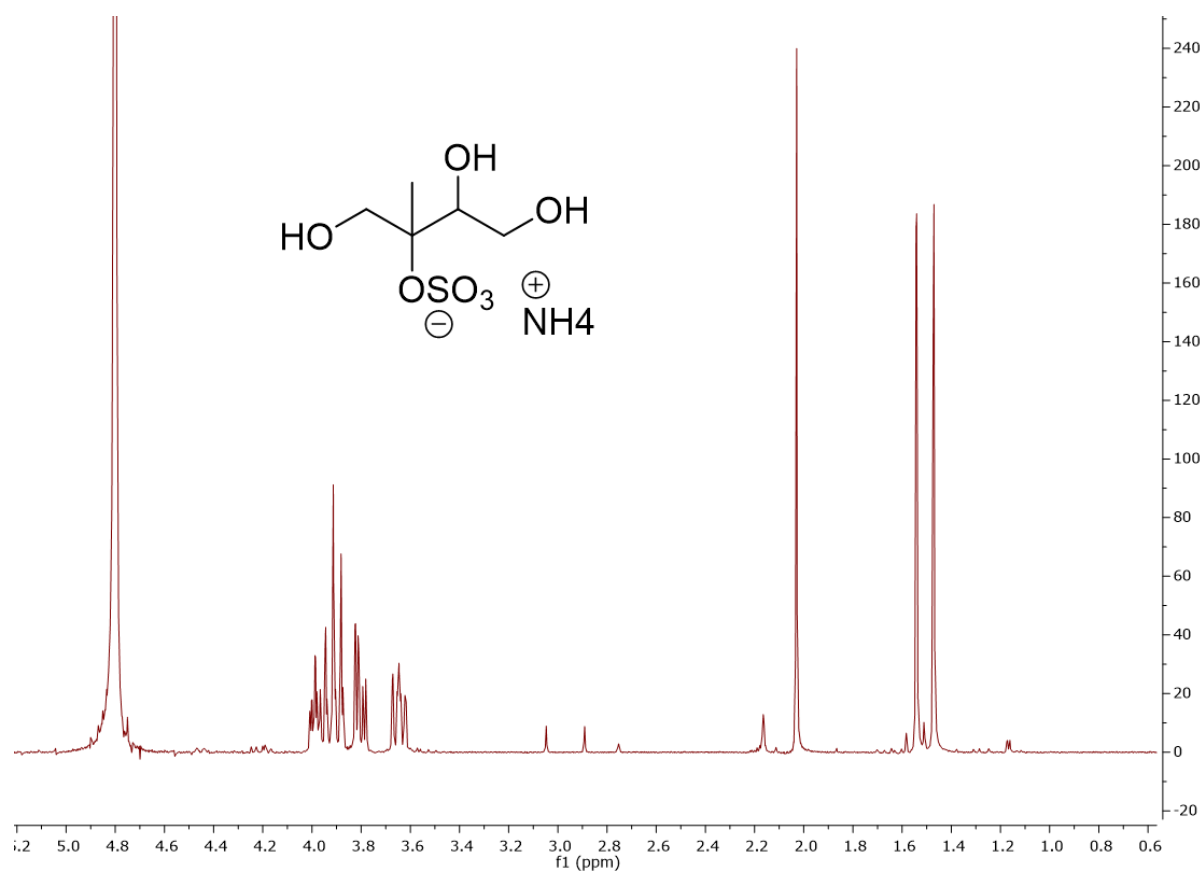


Figure S1. Structure and ¹H NMR (D₂O, 400 MHz) of 2-methyltetrol sulfate (ammonium 1, 3, 4-trihydroxy-2-methylbutan-2-yl sulfate) standard.

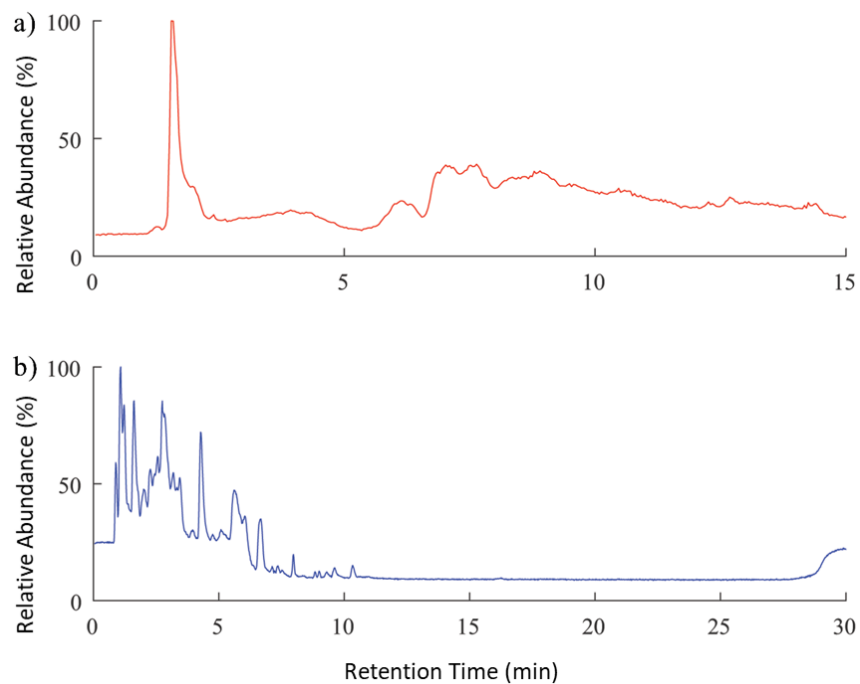


Figure S2. Total ion chromatograms (TICs) of a laboratory-generated β -IEPOX-derived SOA sample separated on **a)** RPLC C₁₈ column, and **b)** HILIC BEH amide column.

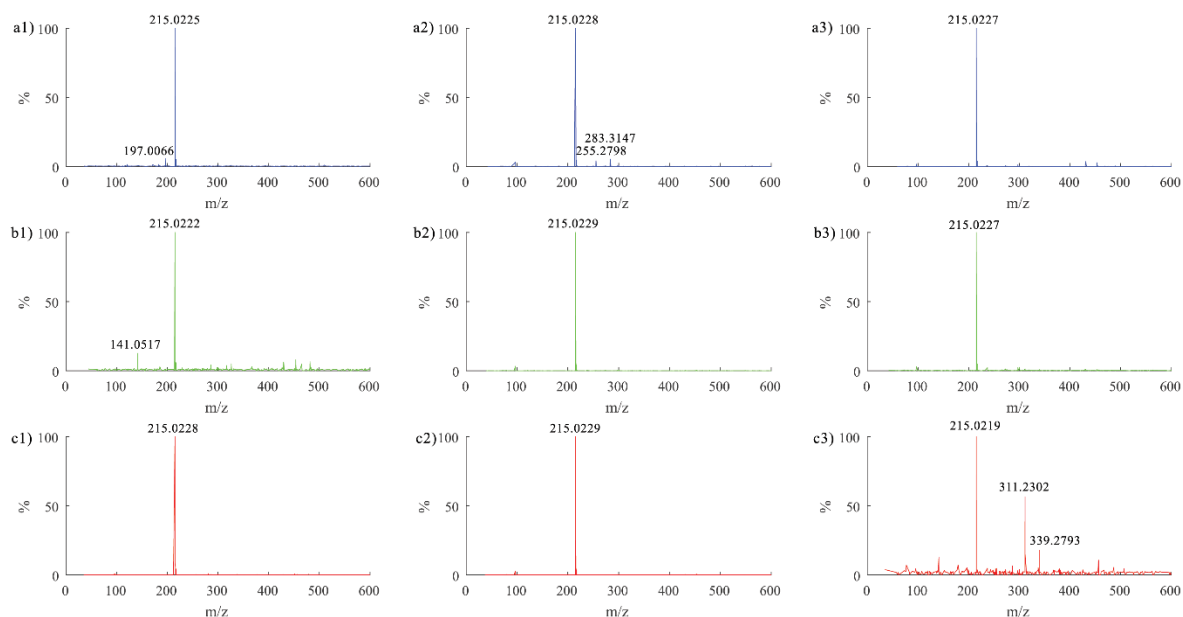


Figure S3. Mass spectra from RPLC/ESI-HR-QTOFMS of the chromatographic peak of m/z 215.023 from **a)** $10 \mu\text{g mL}^{-1}$ standard of 3-methyltetrol sulfate, **b)** laboratory-generated δ -IEPOX SOA, and **c)** $\text{PM}_{2.5}$ sample collected at Look Rock during 2013 SOAS campaign, at RT at: 1) 2.2 min; 2) 4.5 min; and 3) 9.6 min. Note that the chromatographic peak in “c3” has significantly smaller response rate compared to the other chromatographic peaks.

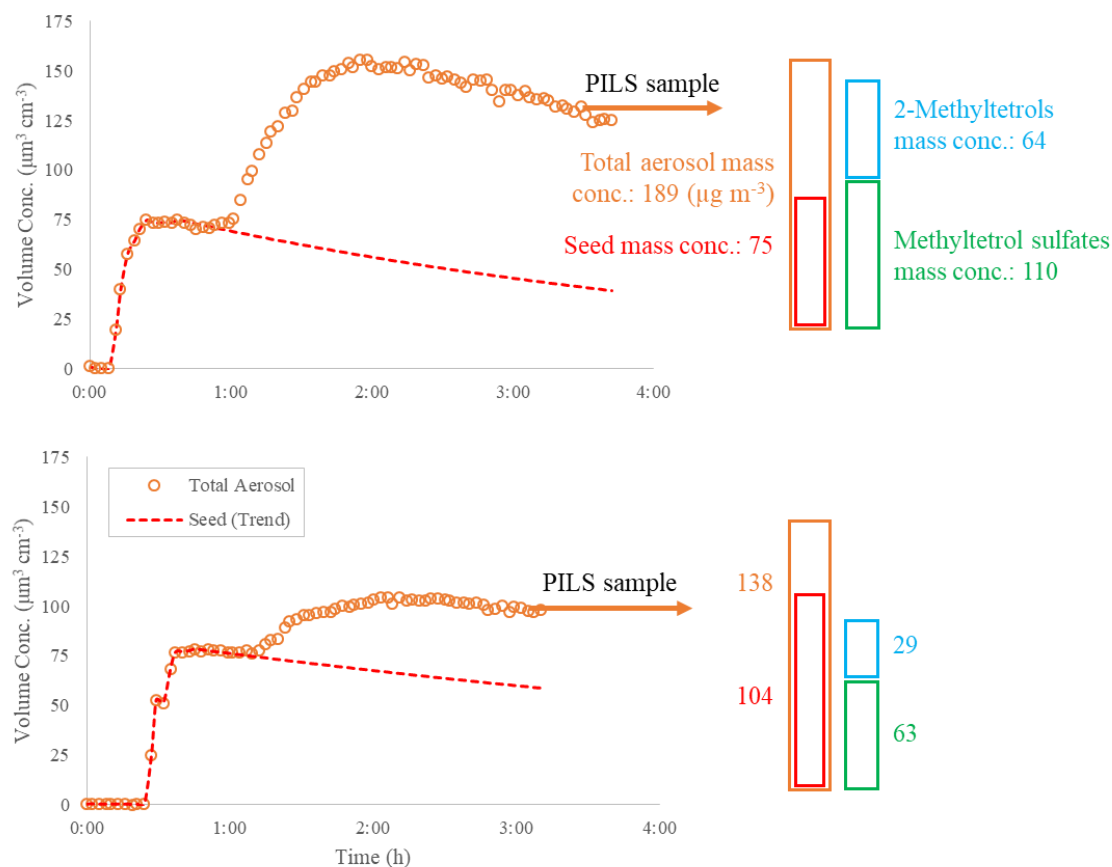


Figure S4. Time profile of total aerosol volume concentration and aerosol mass breakdown for the experiments from (top) *trans*-β-IEPOX; and (bottom) δ -IEPOX. Ammonium bisulfate particles were injected into the chamber to reach $\sim 75 \mu\text{m}^3 \text{cm}^{-3}$. After seed injection, the chamber was left static for at least 30 min to ensure that the seed aerosol was stable and uniformly mixed. Then, 30 mg of *trans*-β- or δ -IEPOX was injected into the chamber. PILS collection was performed at the end of each experiment, as indicated by the arrow. The bars on the right side show the mass concentrations of the total particles, the initial seed particles measured by the SEMS. 2-Methyltetrols and methyltetrol sulfates concentrations were measured by the HILIC/ESI-HR-QTOFMS protocol and indicated by the blue and green bars as well.

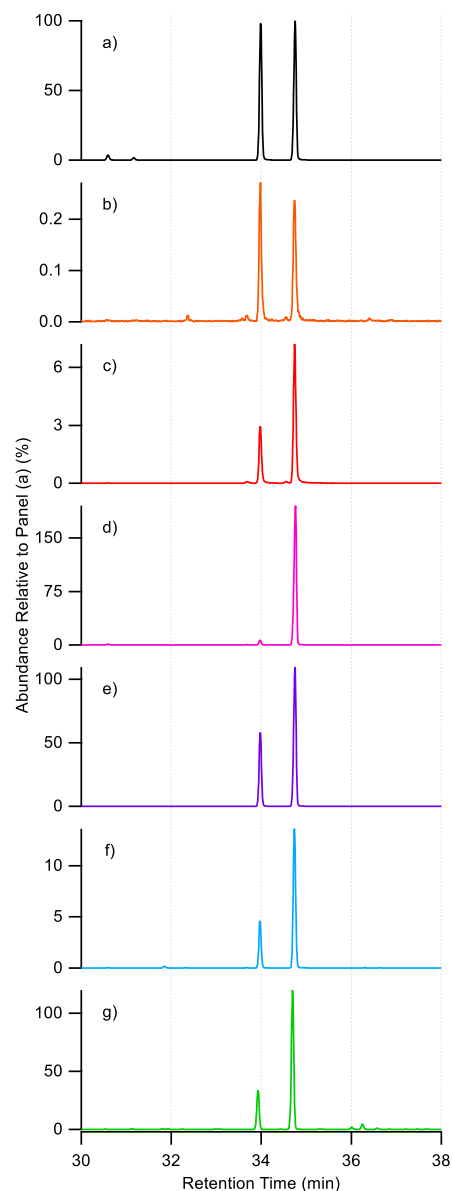


Figure S5. GC/EI-MS EICs of m/z 219 corresponding to 2-methyltetrols (RT = 34.0, 34.8 min) from: **a)** $50 \mu\text{g mL}^{-1}$ standard of 2-methyltetrol; **b)** $50 \mu\text{g mL}^{-1}$ standard of 2-methyltetrol sulfate; **c)** $50 \mu\text{g mL}^{-1}$ standard of 3-methyltetrol sulfate; **d)** laboratory-generated β -IEPOX SOA; **e)** laboratory-generated δ -IEPOX SOA; **f)** $\text{PM}_{2.5}$ sample at Look Rock during 2013 SOAS campaign; **g)** $\text{PM}_{2.5}$ sample at Manaus in Nov. 2016.

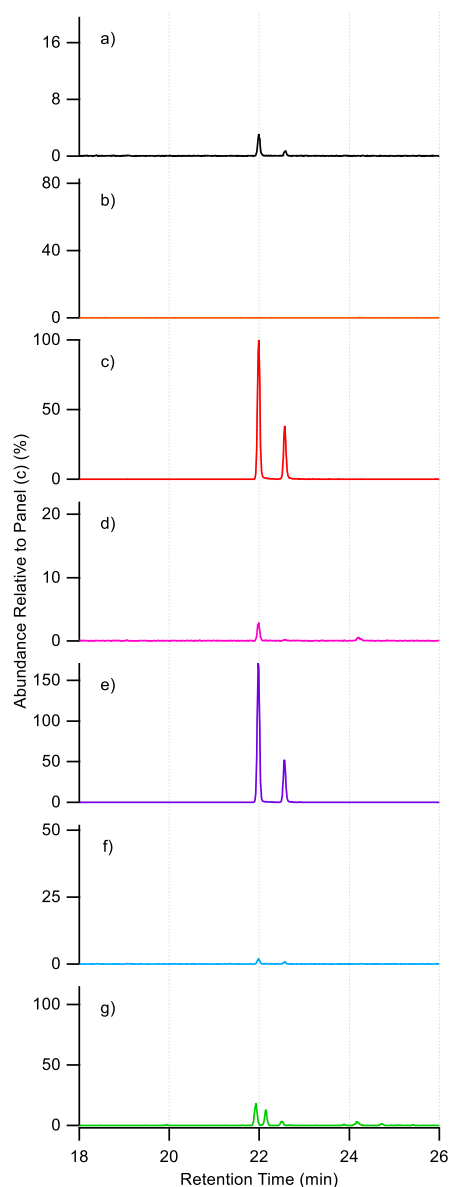


Figure S6. GC/EI-MS EICs of m/z 262 corresponding to 3-MeTHF-3,4-diols (RT = 22.0, 22.6 min) from: **a)** $50 \mu\text{g mL}^{-1}$ standard of 2-methyltetrol; **b)** $50 \mu\text{g mL}^{-1}$ standard of 2-methyltetrol sulfate; **c)** $50 \mu\text{g mL}^{-1}$ standard of 3-methyltetrol sulfate; **d)** laboratory-generated β -IEPOX SOA; **e)** laboratory-generated δ -IEPOX SOA; **f)** $\text{PM}_{2.5}$ sample at Look Rock during 2013 SOAS campaign; **g)** $\text{PM}_{2.5}$ sample at Manaus in Nov. 2016.

APPENDIX 2: SUPPLEMENTARY TABLES AND INFORMATION

Aerosol Mass Calculation and Aerosol Mass Closure for Laboratory-Generated SOA

Chamber aerosol number distributions, which were subsequently converted to total aerosol surface area and volume concentrations, were measured by a scanning electrical mobility system (SEMS v5.0, Brechtel Manufacturing Inc. – BMI) containing a differential mobility analyzer (DMA, BMI) coupled to a mixing condensation particle counter (MCPC Model 1710, BMI). The SEMS system has an internal Nafion dryer connected inline between its inlet and neutralizer. Total aerosol mass concentration was calculated using the total volume concentration multiplied by the density of 1.42 g mL^{-1} of the particles formed after reaction (for the seed aerosol of acidified ammonium sulfate, a density of 1.77 g mL^{-1} was used). The densities used above were reported by Riva et al. based on single-particle characterizations from experiments conducted with *trans*- β -IEPOX and acidified ammonium sulfate aerosols under similar conditions.¹ However, the volume growth was found to be lower for δ -IEPOX-derived SOA, which means the resulting density was higher than 1.42 g mL^{-1} . Therefore, assuming the widely reported organic density of 1.2 g mL^{-1} and volume additivity, the resulting density for total aerosol has been corrected to 1.55 g mL^{-1} , which was used to calculate the mass of total aerosols generated from δ -IEPOX and acidified ammonium sulfate. It is also reasonable to assume that sulfates, either in inorganic or organic forms, remained in the aerosol phase and the change in ammonium equilibrium between the gas and aerosol phase after IEPOX uptake was small as indicated by ACSM measurements. Therefore, the calculated aerosol mass concentration includes both the inorganic sulfate group and the sulfate groups that are covalently bonded to the organic residue. The averaged aerosol masses during the PILS collection periods for the two chamber experiments are shown in Table S1 below.

Table S1. Experimental Conditions and Calculated Aerosol Mass for Laboratory-Generated IEPOX SOA

IEPOX Isomer	Seed Aerosols	Aerosol Mass ($\mu\text{g m}^{-3}$)	Temp ($^{\circ}\text{C}$)	RH (%)
<i>trans</i> - β -IEPOX	$(\text{NH}_4)_2\text{SO}_4 + \text{H}_2\text{SO}_4$	188.51	21-23	50-50
δ -IEPOX	$(\text{NH}_4)_2\text{SO}_4 + \text{H}_2\text{SO}_4$	150.13	21-23	50-55

Figure S4 shows the aerosol volume concentration and the seed volume decay during the experiments. For the laboratory-generated SOA from *trans*- β -IEPOX (top), the PILS sample selected was collected near the end of the experiment at time 3:27 with 2-methyltetrols measured to be $\sim 64 \mu\text{g m}^{-3}$ and methyltetrol sulfates measured to be $\sim 110 \mu\text{g m}^{-3}$. At the same time, the SEMS-MCPC system measured $133 \mu\text{m}^3 \text{cm}^{-3}$ total particle volume concentration, which was converted to a total mass concentration of $189 \mu\text{g m}^{-3}$ (density = 1.42 g mL^{-1}); and $42 \mu\text{m}^3 \text{cm}^{-3}$ seed particle volume concentration (assuming first-order decay rate), which was converted to a total seed mass concentration of $75 \mu\text{g m}^{-3}$ (density = 1.77 g mL^{-1}). Thus, the two quantified IEPOX SOA components accounted for $\sim 92\%$ of the total aerosol mass, which suggests that the inorganic sulfate in the seed aerosol might be substantially converted into organosulfates. A similar mass-closure situation was observed for the laboratory-generated SOA from δ -IEPOX (Figure S6, bottom).

Estimation of C₅-Alkene Triols, 2-Methyltetrols, and 3-MeTHF-3,4-diols Potentially Resulting from Thermal Degradation of Methyltetrol Sulfates

As shown in Figure 5/S4/S5, a large amount of C₅-alkene triols was observed from 2-methyltetrol sulfate standard using GC/EI-MS, while 2-methyltetrols and 3-MeTHF-3,4-diols were observed from 3-methyltetrol sulfate standard. By running both methyltetrol sulfate standards from 0.25-50 $\mu\text{g mL}^{-1}$, we established the semi-quantitative relationship between the response of C₅-alkene triols (as well as 2-methyltetrols and 3-MeTHF-3,4-diols) produced and the concentrations of 2- (or 3-) methyltetrol sulfate standards prepared. For example, the response factor of C₅-alkene triols was determined to be 15301 peak area (in EIC of m/z 231 at 26.9, 27.9, and 28.3 min, see Figure 5) per 1 $\mu\text{g mL}^{-1}$ of 2-methyltetrol sulfate standard. By doing this, as shown in Table S2, we attribute 30.0%, 42.8%, and 14.7% of the C₅-alkene triols to the potential thermal degradation of 2-methyltetrol sulfate from the laboratory-generated SOA from β -IEPOX, the Look Rock, and the Manaus samples, respectively.

Table S2. Estimation of C₅-Alkene Triols due to Thermal Degradation of 2-Methyltetrol Sulfate

	2-Methyltetrol sulfates	C ₅ -Alkene triols corresponding to methyltetrol sulfates	
	$\mu\text{g mL}^{-1}$	$\mu\text{g mL}^{-1}$	%
Lab. SOA from β -IEPOX	355 ^a	1183	30.0%
Look Rock, TN, USA	58	136	42.8%
Manaus, Brazil	175	1185	14.7%

^a The concentrations are converted to the those in the 150- μL solution after reconstitution for the dried filter extracts.

Similarly, the response factors of 2-methyltetrols and 3-MeTHF-3,4-diols were determined to be 5659 and 2169 peak area per 1 $\mu\text{g mL}^{-1}$ of 3-methyltetrol sulfate standard, respectively. Thus, as shown in Table S3, thermal degradation of 3-methyltetrol sulfate might result in 11.1% and over 100% (112.3%) of the 2-methyltetrols and 3-MeTHF-3,4-diols observed in the laboratory-generated SOA from δ -IEPOX.

Table S3. Estimation of 2-Methyltetrols and 3-MeTHF-3,4-diols due to Thermal Degradation of 2-Methyltetrol Sulfate

	3-Methyltetrol sulfates	2-Methyltetrols corresponding to methyltetrol sulfates		3-MeTHF-3,4-diols corresponding to methyltetrol sulfates	
	$\mu\text{g mL}^{-1}$	$\mu\text{g mL}^{-1}$	%	$\mu\text{g mL}^{-1}$	%
Lab. SOA from δ -IEPOX	361 ^a	3247	11.1%	322	112.3%

^a The concentrations are converted to the those in the 150- μL solution after reconstitution for the dried filter extracts.

Note that the concentrations of the measured methyltetrol sulfates (e.g. 355 $\mu\text{g mL}^{-1}$ in Table S2) indicate their concentrations with correction for dilution (40-200 times, see the notes under Table 2) in the 150 μL of solution after reconstitution. The solvent of reconstitution was 95:5 ACN/water for HILIC/ESI-HR-QTOFMS or 2:1 BSTFA/pyridine for GC/EI-MS. The measured concentrations of C₅-alkene triols (as well as 2-methyltetrols and 3-MeTHF-3,4-diols) corresponding to methyltetrol sulfates were also corrected for dilution (by a factor of 4, since only a quarter of the filter content was transferred to GC/EI-MS). Our estimation assumed the same progress of derivatization for the methyltetrol sulfate standards, the laboratory-generated SOA, and the field PM_{2.5} samples, since all of them were analyzed in the same GC/EI-MS worklist.

Analytical Uncertainty

The overall analytical uncertainty, $\%e_T$, in our quantification was calculated using the equation below².

$$\%e_T = \sqrt{\%e_1^2 + \%e_2^2 + \dots + \%e_n^2}$$

When most the (n) relative errors reasonably applied, $\%e_T = \pm 17.2\%$. The relative errors are estimated for:

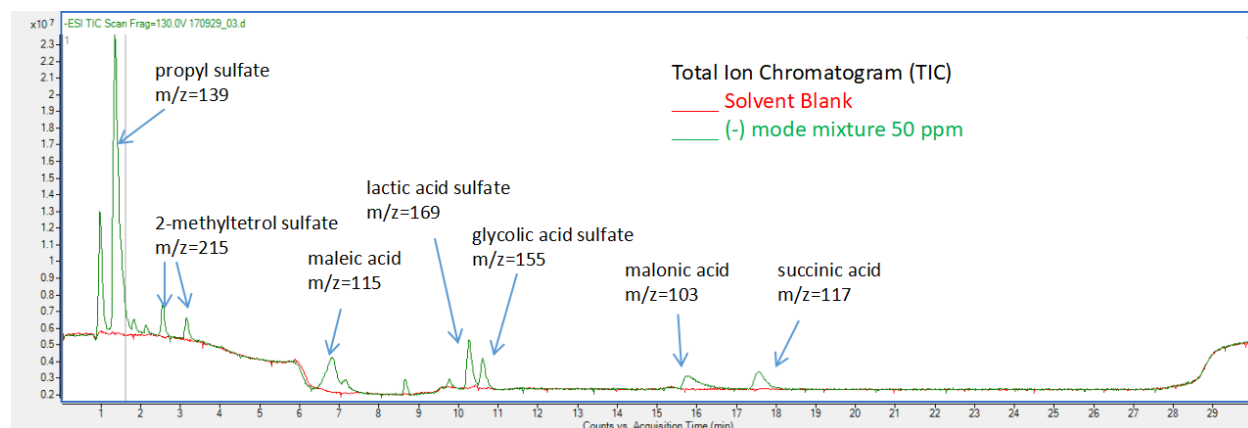
1. Purity of standards and potential degradation over time - $\sim 5\%$, estimated by the internal standard from ^1H NMR and repeated measurements for the same stock standard;
2. Air sampling rate of the filter and PILS samplers - $\sim 0.7\%$, estimated by repeated measurements for the same condition;
3. Water flow rate of PILS wash flow - $\sim 6\%$, estimated by repeated measurements for the same condition;
4. Extraction efficiency (filter) - $\sim 1\%$, the recovery rate of filter extraction using a larger piece of quartz filter (4 cm \times 5 cm, rather than the 47-mm diameter) was determined to be $76.2 \pm 0.8\%$ (for the methyltetrol sulfate standards), but we didn't correct for recovery;
5. Collection efficiency (PILS) - $\sim 2\%$, reported by BMI and examined by comparing the PILS-IC and SEMS-MCPC measurements;
6. Dilution of samples (when needed) - $\sim 1\%$ estimated by the errors caused by transferring liquids;
7. SEMS-MCPC measurement - $\sim 5\%$;
8. Density of IEPOX-SOA particles: $\sim 1\%$;
9. Q-TOF detection - 2% , estimated by relative standard deviation from repeated injections;
10. GC/EI-MS - 2% , estimated by relative standard deviation from repeated injections;
11. Data processing - $\sim 15\%$, this varies by manual integration of chromatographic peak area, selection of linear range of calibration curve, selection of standard for quantification.

References

- (1) Riva, M.; Bell, D. M.; Hansen, A.-M.; Drozd, G. T.; Zhang, Z.; Gold, A.; Imre, D.; Surratt, J. D.; Glasius, M.; Zelenyuk, A. Effect of Organic Coatings, Humidity and Aerosol Acidity on Multiphase Chemistry of Isoprene Epoxydiols. *Environ. Sci. Technol.*, 2016, 5580–8, 50 (11).
- (2) A. P. S. Hettiyadura, T. Jayarathne, K. Baumann, A. H. Goldstein, J. A. de Gouw, A. Koss, F. N. Keutsch, K. Skog, and E. A. Stone, Qualitative and quantitative analysis of atmospheric organosulfates in Centreville, Alabama, *Atmos. Chem. Phys.*, 2017, 17, 1343–1359.

APPENDIX 3: METHOD DEVELOPMENT PROCEDURE

A suite of hydrophilic authentic standards with various chemical structures and polarities were selected to perform the initial development of the method. The suite of standards include four organic acids: oxalic acid, maleic acid, malonic acid and succinic acid, and four organosulfates: propyl sulfate, 2-methyltetrol sulfate, glycolic acid sulfate and lactic acid sulfate. In preparation of the standard solution, 100 mg of each compound was dissolved in 10 ml of solvent. This solution was then diluted for 200 times to make 50 ppm solution. During the optimization process we adjusted various parameters of the method, including sample concentration, organic mobile phase, solvent of standards, pH of the mobile phase, chromatography column, flow rate, aqueous phase gradient and running time. The optimized method for separation of the standards is similar to the method described in the manuscript, with only slight changes on the gradients of the mobile phases. The gradient of organic mobile phase was held constant from 0 min to 2 min at 100%, and then dropped down to 85% from 2 min to 4 min. It was held constant at 85% from 4 min to 25 min before being raised up back to 100% at 26 min. The gradient was then held constant from 26 min to 30 min. The separation can be seen in the figure below:



Seven out of the eight selected compounds were clearly differentiated from the solvent blank and were resolved into clear singlet peaks on the TIC figure, while oxalic acid remained undetected. The separation result of this method was satisfying for the suite of authentic compounds as we moved on to analyze POA and SOA samples with the method.

APPENDIX 4: ABSTRACT PROTOCOL OF HILIC/ESI-HR-QTOFMS METHOD

Sample Preparation

1. Place a filter that you wish to analyze into a 20-mL vial. Submerge the filter with ~20ml of methanol.
2. Put the vial into the sonicator to sonicate for 25 minutes. Change the water in the sonicator and restart the sonicator for another 20 minutes. Take the vial out after sonication.
3. Use a filtered syringe to transfer the liquid solution into a new 20-mL vial.
4. Dry the methanol in the vial with gentle N₂ flow. Lower down the needle in approximately every 30 minutes to make sure the flow is constant. This full drying process might take 7-8 hours.
5. After the vial is fully dried, replace the vial from the dryer. Add 150µL of 95:5 Acetonitrile/H₂O solvent mixture into the vial. Shake the vial so that everything remained in the vial gets fully dissolved in the solvent.
6. Estimate how much dilution you need to do to make sure the amount of target compounds in the sample falls into the linear dynamic range of the prepared standards. If you do not need further dilution to your sample, simply transfer the 150µL solution with a disposable glass pipet into a small brown vial with a glass insert. If you need dilution, inject a small amount of the reconstituted solution into a new small brown vial and dilute with 95:5 Acetonitrile/H₂O solvent mixture. (i.e. For 20x dilution, inject 50µL of the sample solution into the vial and dilute with 950µL of 95:5 Acetonitrile/H₂O solvent mixture. If the final volume of solution is smaller than 300µL, use a glass insert in the vial.

7. Store the sample vial in the -20 °C freezer until the day of analysis.

Standard Preparation

1. Select standard compounds that you wish to target in the sample from chemical inventory in the lab.
2. Weigh out a specific mass (i.e. 10mg) of each standard compound and put it into a new vial. Add a specific volume (i.e. 1mL) of Milli-Q water into the vial to make a high-concentration (i.e. 10,000 ppm) stock solution and make sure all standards are fully dissolved. (assuming all standards are water-soluble)
3. Dilute the solution with 95:5 acetonitrile/H₂O solvent mixture to make a ladder of calibration curve with various concentrations (i.e. 0.01ppm, 0.1ppm, 0.25ppm, 1ppm, 2.5ppm, 10ppm and 25ppm) in small brown vials.
4. Store the vials in the -20 °C freezer until the day of analysis.

Mobile Phase Preparation

1. For mobile phase A (aqueous mobile phase), weigh out 0.5g of solid ammonium acetate compound and put it into a 500-mL volumetric flask. Add Milli-Q water into the volumetric flask and fully dissolve the solid. Keep adding Milli-Q water until the lower surface of the solution reaches the line on the volumetric flask.
2. For mobile phase B (organic mobile phase), weigh out 0.5g of solid ammonium acetate compound and put it into a 500-mL volumetric flask. Add 25mL of Milli-Q water into the volumetric flask and fully dissolve the solid. Add acetonitrile until the lower surface of the solution reaches the line on the volumetric flask.

3. After you make the solution with the volumetric flask, transfer the solution to the mobile phase bottle with the correct label. You do not have to throw out the remaining solution in the bottle.
4. Add small amount of ammonium hydroxide solution step by step into the mobile phase bottle and test the pH value of the solution with pH stripes or pH meter. Keep adding until the pH of the solution reaches approximately 9.

HILIC/ESI-HR-QTOFMS Analysis

1. Carry your prepared sample vials, mobile phase A (water + 0.1% ammonium acetate, pH adjusted to 9 with NH_4OH), mobile phase B (95:5 ACN/ H_2O + 0.1% ammonium acetate, pH adjusted to 9 with NH_4OH), a bottle of solvent mixture of 95:5 ACN/ H_2O and the negative ion mode reference bottle to the mass spec lab located in Rosenau Hall.
2. Find the Waters ACQUITY UPLC BEH Amide column (2.1 \times 100 mm, 1.7 μm particle size) in the mass spec lab and attach the column to the Q-TOF instrument.
3. Attach mobile phase A (aqueous mobile phase) to tubed cap A1. Attach mobile phase B (organic mobile phase) to tubed cap B1. Attach the bottle of 95:5 ACN/ H_2O solvent mixture to tubed cap B2.
4. If you do not wish to do MS/MS analysis, open the method “surratt-method-neg-HILIC-Stack-Burn-MS1_171104.m” in the method folder under Surratt folder. If you do wish to do MS/MS analysis, open the method “Surratt-method-neg-HILIC-Galapagos-MS2_180504.m” in the method folder under Surratt folder.

5. Clean the ESI inlet with methanol and water. Examine the whole route of sample flow and reconnect the if necessary (check out the correct connection on the photo in the group google drive).
6. Turn the pump to waste. Under “binary pump” tab, set the mixture to be 50% mobile phase A/ 50% mobile phase B. Set the flow rate of the pump to be 2mL/min and click “apply”. Keep purging the pump for at least 10 minutes (this can be done at the same time as you tune the instrument).
7. Tune the instrument according to the instruction of mass spec lab technicians.
8. After tuning, go back to the acquisition mode. Go to MS Q-TOF and select the Ref Mass tab. Click “use bottle A” bottle to deliver solution from the reference bottle. Switch bottle B to solvent blank.
9. Set the pump flow rate to 0.2mL/min and composition to 0% of mobile phase B1. After you click apply, turn the knob on to send flow to the LC column.
10. Switch the composition of mobile phase B1 up by 25% every time the pressure has been stabilized for at least 5 minutes. The estimated trend of pump pressure change after stabilizing would be:

%B	0	25	50	75
Pressure (bar)	480	450	160	120

11. Once the mobile phase composition is 100% B1, set the pump flow rate to be 0.3mL/min. Watch the pressure stabilized for at least 5 minutes before starting your worklist run.

Worklist Entry

1. If you do not wish to do MS/MS analysis, you would want to use the method “surratt-method-neg-HILIC-Stack-Burn-MS1_171104.m” in the method folder under Surratt folder. If you do wish to do MS/MS analysis, you would want to use the method “surratt-method-neg-HILIC-Galapagos-MS2_180504.m” in the method folder under Surratt folder.
2. At the end of your worklist, and one injection of solvent blank with the “surratt-shutdown-neg-ms1.m” method. This will flush the column with the 95:5 ACN/H₂O solvent mixture attached to B2 for two and a half hours before shutting down the system.

REFERENCES

1. Y. H. Wang, Z. R. Liu, J. K. Zhang, B. Hu, D. S. Ji, Y. C. Yu and Y. S. Wang, Aerosol physicochemical properties and implications for visibility during an intense haze episode during winter in Beijing, *Atmos. Chem. Phys.*, **2014**, 15(6), 3205-3215.
2. C. I. Davidson, R. F. Phalen and P. A. Solomon, Airborne particulate matter and human health: a review, *Aerosol Sci. Technol.*, **2005**, 39(8), 737-749.
3. M. C. Jacobson, H. -C. Hansson, K. J. Noone and R. J. Charlson, Organic atmospheric aerosols: review and state of the science, *Rev. Geophys.*, **2000**, 38(2), 267-294.
4. J. L. Jimenez, M. R. Canagaratna, N. M. Donahue, A. S. H. Prevot, Q. Zhang, J. H. Kroll, P. F. DeCarlo, J. D. Allan, H. Coe, N. L. Ng, A. C. Aiken, K. S. Docherty, I. M. Ulbrich, A. P. Grieshop, A. L. Robinson, J. Duplissy, J. D. Smith, K. R. Wilson, V. A. Lanz, C. Hueglin, Y. L. Sun, J. Tian, A. Laaksonen, T. Raatikainen, J. Rautiainen, P. Vaattovaara, M. Ehn, M. Kulmala, J. M. Tomlinson, D. R. Collins, M. J. Cubison¹, E. J. Dunlea, J. A. Huffman, T. B. Onasch, M. R. Alfarra, P. I. Williams, K. Bower, Y. Kondo, J. Schneider, F. Drewnick, S. Borrmann, S. Weimer, K. Demerjian, D. Salcedo, L. Cottrell, R. Griffin, A. Takami, T. Miyoshi, S. Hatakeyama, A. Shimono, J. Y. Sun, Y. M. Zhang, K. Dzepina, J. R. Kimmel, D. Sueper, J. T. Jayne, S. C. Herndon, A. M. Trimborn, L. R. Williams, E. C. Wood, A. M. Middlebrook, C. E. Kolb, U. Baltensperger and D. R. Worsnop, Evolution of organic aerosols in the atmosphere, *Science (Washington, DC)*, **2009**, 326(5959), 1525-1529.
5. K. S. Docherty, E. A. Stone, I. M. Ulbrich, P. F. DeCarlo, D. C. Snyder, J. J. Schauer, R. E. Peltier, R. J. Weber, S. M. Murphy, J. H. Seinfeld, B. D. Grover, D. J. Eatough and J. L. Jimenez, Apportionment of primary and secondary organic aerosols in Southern California during the 2005 study of organic aerosols in Riverside (SOAR-1), *Environ. Sci. Technol.*, **2008**, 42, 7655-7662.
6. A. Guenther, T. Karl, P. Harley, C. Wiedinmyer, P. I. Palmer, and C. Geron, Estimates of global terrestrial isoprene emissions using MEGAN (Model of Emissions of Gases and Aerosols from Nature), *Atmos. Chem. Phys.*, **2006**, 6, 3181-3210.
7. W. L. Chameides, R. W. Lindsay, J. Richardson, and C. S. Kiang, The role of biogenic hydrocarbons in urban photochemical smog: Atlanta as a case study, *Science (Washington DC)*, **1988**, 241(4872), 1473-1475.
8. J. D. Surratt, S. M. Murphy, J. H. Kroll, N. L. Ng, L. Hildebrandt, A. Sorooshian, R. Szmigielski, R. Vermeylen, W. Maenhaut, M. Claeys, R. C. Flagan, and J. H. Seinfeld, Chemical composition of secondary organic aerosol formed from the photooxidation of isoprene, *J. Phys. Chem. A*, **2006**, 110(31), 9665-9690.

9. Y. -H. Lin, Z. Zhang, K. S. Docherty, H. Zhang, S. H. Budisulistiorini, C. L. Rubitschun, S. L. Shaw, E. M. Knipping, E. S. Edgerton, T. E. Kleindienst, A. Gold, and J. D. Surratt, Isoprene epoxydiols as precursors to secondary organic aerosol formation: acid-catalyzed reactive uptake studies with authentic compounds, *Environ. Sci. Technol.*, **2012**, 46 (1), 200-258.
10. Y. -H. Lin, E. M. Knipping, E. S. Edgerton, S. L. Shaw, and J. D. Surratt, Investigating the influences of SO₂ and NH₃ levels on isoprene-derived secondary organic aerosol formation using conditional sampling approaches, *Atmos. Chem. Phys.*, **2013**, 13(16), 8457-8470.
11. S. H. Budisulistiorini, M. R. Canagaratna, P. L. Croteau, W. J. Marth, K. Baumann, E. S. Edgerton, S. L. Shaw, E. M. Knipping, D. R. Worsnop, J. T. Jayne, A. Gold, and J. D. Surratt, Real-time continuous characterization of secondary organic aerosol derived from isoprene epoxydiols in downtown Atlanta, Georgia, using the Aerodyne aerosol chemical speciation monitor, *Environ. Sci. Technol.*, **2013**, 47(11), 5685-5694.
12. S. H. Budisulistiorini, X. Li, S. T. Bairai, J. Renfro, Y. Liu, Y. J. Liu, K. A. McKinney, S. T. Martin, V. F. McNeill, H. O. T. Pye, A. Nenes, M. E. Neff, E. A. Stone, S. Mueller, C. Knote, S. L. Shaw, Z. Zhang, A. Gold and J. D. Surratt, Examining the effects of anthropogenic emissions on isoprene-derived secondary organic aerosol formation during the 2013 Southern Oxidant and Aerosol Study (SOAS) at the Look Rock, Tennessee ground site, *Atmos. Chem. Phys.*, **2015**, 15, 8871-8888.
13. S. H. Budisulistiorini, K. Baumann, E. S. Edgerton, S. T. Bairai, S. Mueller, S. L. Shaw, E. M. Knipping, A. Gold, and J. D. Surratt, Seasonal characterization of submicron aerosol chemical composition and organic aerosol sources in the southeastern United States: Atlanta, Georgia, and Look Rock, Tennessee, *Atmos. Chem. Phys.*, **2016**, 16, 5171-5189.
14. W. Rattanavaraha, K. Chu, S. H. Budisulistiorini, M. Riva, Y. -H. Lin, E. S. Edgerton, K. Baumann, S. L. Shaw, H. Guo, L. King, R. J. Weber, M. E. Neff, E. A. Stone, J. H. Offenberg, Z. Zhang, A. Gold and J. D. Surratt, Assessing the impact of anthropogenic pollution on isoprene-derived secondary organic aerosol formation in PM_{2.5} collected from the Birmingham, Alabama, ground site during the 2013 Southern Oxidant and Aerosol Study, *Atmos. Chem. Phys.*, **2016**, 16, 4897-4914.
15. F. Paulot, J. D. Crounse, H. G. Kjaergaard, A. Kürten, J. M. St. Clair, J. H. Seinfeld and P. O. Wennberg, Unexpected Epoxide Formation in the Gas-Phase Photooxidation of Isoprene, *Science*. **2009**, Aug 7; 325(5941):730-3.
16. K. H. Bates, J. D. Crounse, J. M. St. Clair, N. B. Bennett, T. B. Nguyen, J. H. Seinfeld, B. M. Stoltz, and P. O. Wennberg, Gas Phase Production and Loss of Isoprene Epoxydiols, *J. Phys. Chem. A*, **2014**, 118 (7), 1237-1246.
17. W. Wang, I. Kourtchev, B. Graham, J. Cafmeyer, W. Maenhaut, M. Claeys, Characterization of oxygenated derivatives of isoprene related to 2-methyltetrols in Amazonian aerosols using trimethylsilylation and gas chromatography/ion trap mass spectrometry, *Rapid Commun. Mass Spectrom.* **2005**; 19: 1343-1351.

18. J. D. Surratt, A. W. H. Chan, N. C. Eddingsaas, M. Chan, C. L. Loza, A. J. Kwan, S. P. Hersey, R. C. Flagan, P. O. Wennberg and J. H. Seinfeld, Reactive intermediates revealed in secondary organic aerosol formation from isoprene, *Proc. Natl. Acad. Sci. U. S. A*, **2010**, 107(15), 6640-6645.
19. J. D. Surratt, M. Lewandowski, J. H. Offenberg, M. Jaoui, T. E. Kleindienst, E. O. Edney and J. H. Seinfeld, Effect of acidity on secondary organic aerosol formation from isoprene, *Environ. Sci. Technol.*, **2007**, 41(15), 6640-6645.
20. J. D. Surratt, Y. Gomez-Gonzalez, A. W. H. Chan, R. Vermeylen, M. Shahgholi, T. E. Kleindienst, E. O. Edney, J. H. Offenberg, M. Lewandowski, M. Jaoui, W. Maenhaut, M. Claeys, R. C. Flagan, and J. H. Seinfeld, Organosulfate formation in biogenic secondary organic aerosol, *J. Phys. Chem. A*, **2008**, 112, 8345–8378.
21. Y. –H. Lin, S. H. Budisulistiorini, K. Chu, R. A. Siejack, H. Zhang, M. Riva, Z. Zhang, A. Gold, K. E. Kautzman and J. D. Surratt, Light-absorbing oligomer formation in secondary organic aerosol from reactive uptake of isoprene epoxydiols, *Environ. Sci. Technol.*, **2014**, 48(20), 12012-12021.
22. C. J. Gaston, T. P. Riedel, Z. Zhang, A. Gold, J. D. Surratt and J. A. Thornton, Reactive uptake of an isoprene-derived epoxydiol to submicron aerosol particles, *Environ. Sci. Technol.*, **2014**, 48(19), 11178-11186.
23. T. P. Riedel, Y. -H. Lin, S. H. Budisulistiorini, C. J. Gaston, J. A. Thornton, Z. Zhang, W. Vizuite, A. Gold, and J. D. Surratt, Heterogeneous reactions of isoprene-derived epoxides: Reaction probabilities and molar secondary organic aerosol yield estimates, *Environ. Sci. Technol. Lett.*, **2015**, 2(2), 38-42.
24. M. Claeys, B. Graham, G. Vas, W. Wang, R. Vermeylen, V. Pashynska, J. Cafmeyer, P. Guyon, M. O. Andreae, P. Artaxo, W. Maenhaut, Formation of secondary organic aerosols through photooxidation of isoprene, *Science (Washington DC)*, **2004**, 303(5661), 1173-1176.
25. F. D. Lopez-Hilfiker, C. Mohr, E. L. D'Ambro, A. Lutz, T. P. Riedel, C. J. Gaston, S. Iyer, Z. Zhang, A. Gold, J. D. Surratt, B. H. Lee, T. Kurten, W.W. Hu, J. Jimenez, M. Hallquist, and J. A. Thornton, Molecular composition and volatility of organic aerosol in the Southeastern U.S.: implications for IEPOX derived SOA, *Environ. Sci. Technol.* **2016**, 50(5), 2200-2209.
26. G. Isaacman-VanWertz, L. D. Yee, N. M. Kreisberg, R. Wernis, J. A. Moss, S. V. Hering, S. de Sa, S. T. Martin, M. L. Alexander, B. B. Palm, W. Hu, P. Campuzano-Jost, D. A. Day, J. L. Jimenez, M. Riva, J. D. Surratt, J. Viegas, A. Manzi, E. Edgerton, K. Baumann, R. Souza, P. Artaxo, and A. H. Goldstein, Ambient Gas-Particle Partitioning of Tracers for Biogenic Oxidation, *Environ. Sci. Technol.*, **2016**, 50 (18), 9952–9962.

27. G. Isaacman, N. M. Kreisberg, L. D. Yee, D. R. Worton, A. W. H. Chan, J. A. Moss, S. V. Hering, A. H. Goldstein, Online derivatization for hourly measurements of gas- and particle-phase semi-volatile oxygenated organic compounds by thermal desorption aerosol gas chromatography (SV-TAG), *Atmos. Meas. Tech.*, **2014**, 7(12), 4417-4429.
28. Y. Gomez-Gonzalez, J. D. Surratt, F. Cuyckens, R. Szmigelski, R. Vermeylen, M. Jaoui, M. Lewandowski, J. H. Offenberg, T. E. Kleindienst, E. O. Edney, F. Blockhuys, C. Van Alsenoy, W. Maenhaut and M. Claeys, Characterization of organosulfates from the photooxidation of isoprene and unsaturated fatty acids in ambient aerosol using liquid chromatography/ (–) electrospray ionization mass spectrometry, *J. Mass Spectrom.*, **2008**, 43, 371-382.
29. A. J. Alpert, Hydrophilic-interaction chromatography for the separation of peptides, nucleic acids and other polar compounds, *J. Chromatogr., A*, **1990**, 499(19), 177-196.
30. A. P. S. Hettiyadura, E. A. Stone, S. Kundu, Z. Baker, E. Geddes, K. Richards, and T. Humphry, Detection of atmospheric organosulfates using HILIC chromatography with MS detection, *Atmos. Meas. Tech.*, **2015**, 8, 2347-2358.
31. G. Spolnik, P. Wach, K. J. Rudzinski, K. Skotak, W. Danikiewicz, and R. Szmigielski, Improved UHPLC-MS/MS methods for analysis of isoprene-derived organosulfates, *Anal. Chem.*, **2018**, 90 (5), 3416–3423.
32. A. P. S. Hettiyadura, T. Jayarathne, K. Baumann, A. H. Goldstein, J. A. de Gouw, A. Koss, F. N. Keutsch, K. Skog, and E. A. Stone, Qualitative and quantitative analysis of atmospheric organosulfates in Centreville, Alabama, *Atmos. Chem. Phys.*, **2017**, 17, 1343–1359.
33. P. Jandera, (2008). Stationary phases for hydrophilic interaction chromatography, their characterization and implementation into multidimensional chromatography concepts, *J. Sep. Sci.*, **2008**, 31(9), 1421-1437.
34. P. Hemstrom and K. Irgum, Hydrophilic interaction chromatograph, *J. Sep. Sci.*, **2006**, 29(12), 1784-1821.
35. Y. Guo and S. Gaiki, Retention behavior of small polar compounds on polar stationary phases in hydrophilic interaction chromatography, *J. Chromatogr., A*, **2005**, 1074(1–2), 71-80.
36. H. O. T. Pye, R. W. Pinder, I. R. Piletic, Y. Xie, S. L. Capps, Y. –H. Lin, and E. O. Edney, (2013). Epoxide pathways improve model predictions of isoprene markers and reveal key role of acidity in aerosol formation, *Environ. Sci. Technol.*, **2013**, 47(19), 11056-11064.
37. V. F. McNeill, Aqueous organic chemistry in the atmosphere: sources and chemical processing of organic aerosols, *Environ. Sci. Technol.*, **2015**, 49(3), 1237-1244.

38. E. A. Marais, D. J. Jacob, J. L. Jimenez, P. Campuzano-Jost, D. A. Day, W. Hu, J. Krechmer, L. Zhu, P. S. Kim, C. C. Miller, J. A. Fisher, K. Travis, K. Yu, T. F. Hanisco, G. M. Wolfe, H. L. Arkinson, H. O. T. Pye, K. D. Froyd, J. Liao and V. F. McNeill. Aqueous-phase mechanism for secondary organic aerosol formation from isoprene: application to the southeast United States and co-benefit of SO₂ emission controls, *Atmos. Chem. Phys.*, **2016**, 16(3), 1603-1618.
39. S. H. Budisulistiorini, A. Nenes, A. G. Carlton, J. D. Surratt, V. F. McNeill, and H. O. T. Pye, Simulating aqueous-phase isoprene-epoxydiol (IEPOX) secondary organic aerosol production during the 2013 southern oxidant and aerosol study (SOAS), *Environ. Sci. Technol.*, **2017**, 51(9), 5026-5034.
40. A. L. Bondy, R. L. Craig, Z. Zhang, A. Gold, J. D. Surratt, and A. P. Ault, Isoprene-derived organosulfates: vibrational mode analysis by Raman spectroscopy, acidity-dependent spectral modes, and observation in individual atmospheric particles, *J. Phys. Chem. A*, **2018**, 122 (1), 303–315.
41. Z. Zhang, Y. –H. Lin, J. D. Surratt, L. M. Ball, A. Gold, Technical Note: Synthesis of isoprene atmospheric oxidation products: isomeric epoxydiols and the rearrangement products *cis* and *trans*-3-methyl-3,4-dihydroxytetrahydrofuran. *Atmos. Chem. Phys.*, **2012**, 12, 8529–8535.
42. H. Zhang, J. D. Surratt, Y. H. Lin, J. Bapat, and R. M. Kamens, Effect of relative humidity on SOA formation from isoprene/NO photooxidation: enhancement of 2-methylglyceric acid and its corresponding oligoesters under dry conditions, *Atmos. Chem. Phys.*, **2011**, 11, 6411-6424.
43. J. E. Krechmer, M. Groessl, X. Zhang, H. Junninen, P. Massoli, A. T. Lambe, J. R. Kimmel, M. J. Cubison, S. Graf, Y.-H. Lin, S. H. Budisulistiorini, H. Zhang, J. D. Surratt, R. Knochenmuss, J. T. Jayne, D. R. Worsnop, J.-L. Jimenez, and M. R. Canagaratna, Ion mobility spectrometry–mass spectrometry (IMS–MS) for on- and offline analysis of atmospheric gas and aerosol species, *Atmos. Meas. Tech.*, **2016**, 9, 3245–3262.
44. S. S. de Sá B. B. Palm, P. Campuzano-Jost, D. A. Day, M. K. Newburn, W. Hu, G. Isaacman-VanWertz, L. D. Yee, R. Thalman, J. Brito, S. Carbone, P. Artaxo, A. H. Goldstein, A. O. Manzi, R. A. F. Souza, F. Mei, J. E. Shilling, S. R. Springston, J. Wang, J. D. Surratt, M. L. Alexander, J. L. Jimenez, and S. T. Martin, Influence of urban pollution on the production of organic particulate matter from isoprene epoxydiols in central Amazonia, *Atmos. Chem. Phys.*, **2017**, 17, 6611–6629.
45. T. B. Nguyen, G. S. Tyndall, J. D. Crounse, A. P. Teng, K. H. Bates, R. H. Schwantes, M. M. Coggon, L. Zhang, P. Feiner, D. O. Milller, K. M. Skog, J. C. Rivera-Rios, M. Dorris, K. F. Olson, A. Koss, R. J. Wild, S. S. Brown, A. H. Goldstein, J. A. de Gouw, W. H. Brune, F. N. Keutsch, J. H. Seinfeld and P. O. Wennberg, Atmospheric fates of Criegee intermediates in the ozonolysis of isoprene, *Phys. Chem. Chem. Phys.*, **2016**, 18, 10241-10254.

46. A. Watanabe, S. J. Stropoli, and M. J. Elrod, Assessing the Potential Mechanisms of Isomerization Reactions of Isoprene Epoxydiols on Secondary Organic Aerosol, *Environ. Sci. Technol.* Just Accepted Manuscript, **2018**, DOI: 10.1021/acs.est.8b01780
47. V. F. McNeill, J. L. Woo, D. D. Kim, A. N. Schwier, N. J. Wannell, A. J. Sumner, and J. M. Barakat, Aqueous-phase secondary organic aerosol and organosulfate formation in atmospheric aerosols: a modeling study, *Environ. Sci. Technol.*, **2012**, 46 (15), 8075–8081.
48. J. L. Woo and V. F. McNeill, SimpleGAMMA v1.0 – a reduced model of secondary organic aerosol formation in the aqueous aerosol phase (aaSOA), *Geosci. Model Dev.*, **2015**, 8, 1821–1829.
49. H. O. T. Pye, D. J. Luecken, L. Xu, C. M. Boyd, N. L. Ng, K. R. Baker, B. R. Ayres, J. O. Bash, K. Baumann, W. P. L. Carter, E. Edgerton, J. L. Fry, W. T. Hutzell, D. B. Schwede, and P. B. Shepson, Modeling the current and future roles of particulate organic nitrates in the Southeastern United States, *Environ. Sci. Technol.*, **2015**, 49 (24), 14195–14203.
50. L. Wu, G. Broquet, P. Ciais, V. Bellassen, F. Vogel, F. Chevallier, I. Xueref-Remy, and Y. Wang, What would dense atmospheric observation networks bring to the quantification of city CO₂ emissions?, *Atmos. Chem. Phys.*, **2016**, 16, 7743–7771.